ACOUSTIC MODELING STUDY – UNDERWATER SOUND LEVELS FROM MARINE PILE DRIVING IN SOUTHEAST ALASKA

Vibratory pile driving at the Kake Ferry terminal (JASCO Applied Sciences, September 2015).

Prepared By:
Jorge E. Quijano
Melanie E. Austin
Graham A. Warner

Prepared For:
Alaska Department of Transportation & Public Facilities
Research, Development, and Technology Transfer
P.O. Box 112500
3132 Channel Drive
Juneau, Alaska 99811-2500
and
Federal Highway Administration
P.O. Box 21648
709 West 9th Street
Juneau, Alaska 99802-1648

REPORT DOCUMENTATION PAGE

Form approved OMB No.

1. AGENCY USE ONLY (LEAVE BLANK)	2. REPORT DATE	3. REPORT TYPE AND DATES COVERED
4000(135)	July 21, 2017	FINAL, May 2017 – August 2017

4. TITLE AND SUBTITLE
Acoustic Modeling Study – Underwater Sound Levels from Marine Pile Driving in Southeast Alaska

5. FUNDING NUMBERS
Federal # 4000(135)
IRIS # Z6236000

6. AUTHOR(S)
J.E. Quijano, M.E. Austin, and G.J. Warner

7. PERFORMING ORGANIZATION NAME(S) AND ADDRESS(ES)
JASCO Applied Sciences
310 K Street, Suite 200
Anchorage, Alaska 99501

8. PERFORMING ORGANIZATION REPORT NUMBER
4000(135)B

9. SPONSORING/MONITORING AGENCY NAME(S) AND ADDRESS(ES)
Alaska Department of Transportation and Public Facilities
Research, Development &Technology Transfer
3132 Channel Drive
Juneau, Alaska 99811-2500

10. SPONSORING/MONITORING AGENCY REPORT NUMBER
49000(135)B

11. SUPPLEMENTARY NOTES

12a. DISTRIBUTION / AVAILABILITY STATEMENT
Copies available online at http://www.dot.alaska.gov/stwddes/research/search_lib.shtml

12b. DISTRIBUTION CODE

13. ABSTRACT (Maximum 200 words)

JASCO Applied Sciences conducted numerical modeling for Alaska DOT&PF to characterize underwater noise from pile driving activities at four locations in Southeast Alaska. The model was used to calculate source levels and underwater sound footprints for impact and vibratory pile driving at the Auke Bay, Kake, Ketchikan, and Kodiak ferry terminals. Rock socket drilling was also modeled at Kodiak. Model outputs were interpreted to calculate distances from the piles to behavioral disturbance sound pressure level thresholds for each source type and location. Distances to injurious peak and cumulative sound exposure level thresholds were also calculated. Sound exposure levels were frequency-weighted to account for hearing sensitivity of marine mammal groups, in accordance with guidance of the National Marine Fisheries Service. The model results were validated against measured data that JASCO collected at the same sites, during ferry terminal improvement construction projects in 2015 and 2016.

14. KEYWORDS : noise, maritime construction, numerical modeling, pile driving

15. NUMBER OF PAGES
70

16. PRICE CODE
N/A

17. SECURITY CLASSIFICATION OF REPORT	18. SECURITY CLASSIFICATION OF THIS PAGE	19. SECURITY CLASSIFICATION OF ABSTRACT	20. LIMITATION OF ABSTRACT
Unclassified	Unclassified	Unclassified	None

Notice

This document is disseminated under the sponsorship of the U.S. Department of Transportation in the interest of information exchange. The U.S. Government assumes no liability for the use of the information contained in this document.

The U.S. Government does not endorse products or manufacturers. Trademarks or manufacturers' names appear in this report only because they are considered essential to the objective of the document.

Quality Assurance Statement

The Federal Highway Administration (FHWA) provides high-quality information to serve Government, industry, and the public in a manner that promotes public understanding. Standards and policies are used to ensure and maximize the quality, objectivity, utility, and integrity of its information. FHWA periodically reviews quality issues and adjusts its programs and processes to ensure continuous quality improvement.

Author's Disclaimer

Opinions and conclusions expressed or implied in the report are those of the author. They are not necessarily those of the Alaska DOT&PF or funding agencies.

SI* (MODERN METRIC) CONVERSION FACTORS

APPROXIMATE CONVERSIONS TO SI UNITS

Symbol	When You Know	Multiply By	To Find	Symbol
		LENGTH		
in	inches	25.4	millimeters	
	mm ft	feet		
	0.305	meters	m yd	
	yards	0.914	meters	m
		AREA		
in^2	square inches	645.2	square millimeters	
	$mm^{2\ ft2}$	square feet		0.093
	square meters	m^2 yd^2	square yard	
	0.836	square meters	m^2	
ac	acres	0.405	hectares	ha
		VOLUME		
fl oz	fluid ounces	29.57	milliliters	mL
gal	gallons	3.785	liters	
	L ft^3	cubic feet	0.028	
	cubic meters	m^3 yd^3	cubic yards	
	0.765	cubic meters	m^3	
		MASS		
oz	ounces	28.35	grams	g
lb	pounds	0.454	kilograms	kg
T	short tons (2000 lb)	0.907	megagrams (or "metric ton")	Mg (or "t")
		TEMPERATURE (exact degrees)		
°F	Fahrenheit	5 (F-32)/9 or (F-32)/1.8	Celsius	°C
		ILLUMINATION		
fc	foot-candles	10.76	lux	lx
fl	foot-Lamberts	3.426	$candela/m^2$	cd/m^2
		FORCE and PRESSURE or STRESS		
lbf	poundforce	4.45	newtons	N
lbf/in^2	poundforce per square inch	6.89	kilopascals	kPa

APPROXIMATE CONVERSIONS FROM SI UNITS

Symbol	When You Know	Multiply By	To Find	Symbol
		LENGTH		
mm	millimeters	0.039	inches	in
m	meters	3.28	feet	ft
m	meters	1.09	yards	yd
km	kilometers	0.621	miles	mi
		AREA		
mm^{2} square millimeters 0.0016 square inches $in^{2\ m2}$ square meters 10.764 square feet $ft^{2\ m2}$ square meters 1.195 square yards yd^2				
ha hectares 2.47 acres ac km^2 square kilometers 0.386 square miles mi^2				
		VOLUME		
mL	milliliters	0.034	fluid ounces	fl oz
L	liters	0.264	gallons	gal
m^3	cubic meters	35.314	cubic feet	$ft^{3\ m3}$
	cubic meters	1.307	cubic yards	yd^3
		MASS		
g	grams	0.035	ounces	oz
kg	kilograms	2.202	pounds	lb
Mg (or "t")	megagrams (or "metric ton")	1.103	short tons (2000 lb)	T
		TEMPERATURE (exact degrees)		
°C	Celsius	1.8C+32	Fahrenheit	°F
		ILLUMINATION		
lx	lux	0.0929	foot-candles	fc
cd/m^2	$candela/m^2$	0.2919	foot-Lamberts	fl
		FORCE and PRESSURE or STRESS		
N	newtons	0.225	poundforce	lbf
kPa	kilopascals	0.145	poundforce per square inch	lbf/in^2

*SI is the symbol for the International System of Units. Appropriate rounding should be made to comply with Section 4 of ASTM E380.
(Revised March 2003)

Suggested citation:

Quijano, J. M. Austin and G. Warner. 2017. Acoustic Modeling Study: Underwater Sound Levels from Marine Pile Driving in Southeast Alaska. JASCO Document 01429, Version 1.0. Technical report by JASCO Applied Sciences for Alaska Department of Transportation and Public Facilities. Report No 4000(135)B.

Disclaimer:

The results presented herein are relevant within the specific context described in this report. They could be misinterpreted if not considered in the light of all the information contained in this report. Accordingly, if information from this report is used in documents released to the public or to regulatory bodies, such documents must clearly cite the original report, which shall be made readily available to the recipients in integral and unedited form.

Contents

EXECUTIVE SUMMARY 1
1. INTRODUCTION 2
2. METHODS 3
2.1. Modeling Source Sound Levels with PDSM 3
2.2. Comparing Modeled Levels to Measurements with FWRAM 4
2.3. Modeling Ranges to Marine Mammal Impact Thresholds 4
2.3.1. Estimating SPL from MONM-modeled SEL results 5
2.4. Computing Total Sound Exposure Levels 6
3. MODEL PARAMETERS 7
3.1. Source Specifications 7
3.2. Bathymetry 8
3.3. Geoacoustic Profiles 8
3.3.1. Geoacoustics for Auke Bay 8
3.3.2. Geoacoustics for Kake 9
3.3.3. Geoacoustics for Ketchikan 9
3.3.4. Geoacoustics for Kodiak 10
4. MODELED SOURCE LEVELS 11
5. COMPARING MODELED AND MEASURED LEVELS 13
5.1. Auke Bay 13
5.2. Kake 15
5.3. Ketchikan 17
5.4. Kodiak 19
6. SOUND LEVEL CONTOURS 22
6.1. Auke Bay 22
6.2. Kake 25
6.3. Ketchikan 28
6.4. Kodiak 31
7. DISTANCES TO CRITERIA THRESHOLDS 36
7.1. Auke Bay 36
7.2. Kake 37
7.3. Ketchikan 37
7.4. Kodiak 38
8. DISCUSSION AND SUMMARY 40
GLOSSARY 42
LITERATURE CITED 47
APPENDIX A. UNDERWATER ACOUSTICS THEORY AND FORMULAE A-1

APPENDIX B. THRESHOLD CRITERIA FOR MARINE MAMMAL INJURY (LEVEL A) AND BEHAVIORAL DISTURBANCE (LEVEL B).....B-1

APPENDIX C. MODELING CONSIDERING HIGH SHEAR VELOCITY IN BEDROCK SUBSTRATE ... C-4

Figures

Figure 1. Sample areas ensonified to an arbitrary sound level with R_{max} and $R_{95\%}$ ranges shown for two different scenarios. 5

Figure 2. Range-dependent conversion factors for converting SEL-to-SPL..... 6

Figure 3. Force at the top of the pile corresponding to (left) impact and (right) vibratory pile driving at the four locations considered in this study. 11

Figure 4. Source levels in 1/3-octave-bands used to model impact and vibratory pile driving at (top left) Auke Bay, (top right) Kake, (bottom left) Ketchikan, and (bottom right) Kodiak. 12

Figure 5 Source levels in 1/3-octave-bands used to model drilling at Kodiak. 12

Figure 6. Auke Bay: Modeled band labels for (left) impact and (right) vibratory pile driving compared to measured band levels (maximum and mean) at the closest measurement range of 7m..... 13

Figure 7. Auke Bay: Comparison of modeled and measured SEL, SPL, and PK levels for (left column) impact and (right column) vibratory pile driving. 14

Figure 8. Kake: Modeled band labels for (left) impact and (right) vibratory pile driving compared to measured band levels (maximum and mean) at the closest measurement range..... 15

Figure 9. Kake: Comparison of modeled and measured SEL, SPL, and PK levels (left column) impact and (right column) vibratory pile driving. 16

Figure 10. Ketchikan: Modeled band labels for (left) impact and (right) vibratory pile driving compared to measured band levels (maximum and mean) at the closest measurement range..... 17

Figure 11. Ketchikan: Comparison of modeled and measured SEL, SPL, and PK levels for (left column) impact and (right column) vibratory pile driving. 18

Figure 12. Kodiak: Modeled band labels for (left) impact and (right) vibratory pile driving compared to measured band levels (maximum and mean) at the closest measurement range of 16 m..... 19

Figure 13. Kodiak Comparison of modeled and measured SEL, SPL, and PK levels (left column) impact and (right column) vibratory pile driving 20

Figure 14. Kodiak: Comparison of modeled and measured SEL for drilling. 21

Figure 15. Auke Bay: Spatial dependency of the modeled SPL for (top) impact and (bottom) vibratory pile driving, ... 22

Figure 16. Auke Bay: Contours to thresholds for marine mammal injury and behavioral disturbance from impulsive sources for impact pile driving. 23

Figure 17. Auke Bay: Contours to thresholds for marine mammal injury (where exceeded) and behavioral disturbance from non-impulsive sources for vibratory pile driving. 24

Figure 18. Kake: Spatial dependency of the modeled SPL for (top) impact and (bottom) vibratory pile driving, ... 25

Figure 19. Kake: Contours to thresholds for marine mammal injury and behavioral disturbance from impulsive sources for impact pile driving. 26

Figure 20. Kake: Contours to thresholds for marine mammal injury (where exceeded) and behavioral disturbance from non-impulsive sources for vibratory pile driving. 27

Figure 21. Ketchikan: Spatial dependency of the modeled SPL for (top) impact and (bottom) vibratory pile driving, ... 28

Figure 22. Ketchikan: Contours to thresholds for marine mammal injury and behavioral disturbance from impulsive sources for impact pile driving. 29

Figure 23. Ketchikan: Contours to thresholds for marine mammal injury (where exceeded) and behavioral disturbance from non-impulsive sources for vibratory pile driving. 30
Figure 24. Kodiak: Spatial dependency of the modeled SPL for (top) impact and (bottom) vibratory pile driving, ... 31
Figure 25. Kodiak: Contours to thresholds for marine mammal injury (where exceeded) and behavioral disturbance from impulsive sources for impact pile driving. 32
Figure 26. Kodiak: Contours to thresholds for behavioral disturbance from non-impulsive sources for vibratory pile driving 33
Figure 27. Kodiak: Contours to thresholds for behavioral disturbance from non-impulsive sources for drilling. 34
Figure 28. Kodiak: Contours to thresholds for marine mammal injury from non-impulsive sources for vibratory pile driving and drilling. 35

Tables

Table 1. Monitored and modeled pile driving activities at the four measurement locations. 7
Table 2. Auke Bay: Geoacoustic properties. 8
Table 3. Kake: Geoacoustic properties. 9
Table 4. Ketchikan: Geoacoustic properties. 9
Table 5. Kodiak: Geoacoustic properties. 10
Table 6. Auke Bay: Distance in meters to SPL thresholds based on NMFS (2013) criteria 36
Table 7. Auke Bay: Range in meters to onset of injury, based on NMFS (2016) criteria. 36
Table 8. Kake: Distance in meters to SPL thresholds, determined from modeling and from best-fit transmission loss coefficient and SPLs at the closest measurement range 37
Table 9. Kake: Range in meters to onset of hearing injury, based on NMFS (2016) criteria. 37
Table 10. Ketchikan: Distance to SPL thresholds, determined from modeling and from best-fit transmission loss coefficient and SPLs at the closest measurement range 37
Table 11. Ketchikan: Range in meters to onset of hearing injury, based on NMFS (2016). 38
Table 12. Kodiak: Distance to SPL thresholds, determined from modeling and from best-fit transmission loss coefficient and SPLs at the closest measurement range 38
Table 13. Kodiak: Range in meters to onset of injury. 39
Table 14 Broadband SPL (dB re 1 μPa^2s) for impact and vibratory pile driving, measured and modeled, at the closest measurement location. 40

Executive Summary

JASCO Applied Sciences conducted numerical modeling for Alaska DOT&PF to characterize underwater noise from pile driving activities at four locations in Southeast Alaska. The model was used to calculate source levels and underwater sound footprints for impact and vibratory pile driving at the Auke Bay, Kake, Ketchikan, and Kodiak ferry terminals. Rock socket drilling was also modeled at Kodiak.

Model outputs were interpreted to calculate distances from the piles to behavioral disturbance sound pressure level thresholds for each source type and location. Distances to injurious peak levels and cumulative sound exposure level thresholds were also calculated. Sound exposure levels were frequency-weighted to account for hearing sensitivity of marine mammal groups, in accordance with guidance of the National Marine Fisheries Service. The model results were validated against measured data that JASCO collected at the same sites, during ferry terminal improvement construction projects in 2015 and 2016.

The model accurately simulated source sound levels for impact and vibratory pile driving when compared to maximum levels from data measured within 7-17 m from the pile. Broadband modeled sound levels trended with the measured data in terms of the decay of the sound levels with range. Because the source model was tuned to replicate the maximum measured sound levels, the models tended to predict longer ranges to the marine mammal impact thresholds than were obtained from an analysis of the empirical data alone. The exception to this was for instances of vibratory pile driving for which the empirical approach yielded unrealistically large distances to the behavioral harassment thresholds, from extrapolations far beyond the farthest measurement distance. In these cases, the model predicted shorter, and more realistic threshold distances for behavioral harassment.

Data at Kodiak were least-well simulated with the model due to effects from the interaction of the sound waves with the consolidated bedrock at the seafloor at that location, which were not accurately simulated by the models. This effected a small band of frequencies, and resulted in a small overestimation of the modeled levels for Kodiak. Sound levels at Kodiak could be more accurately simulated with a different propagation model that fully treats shear wave propagation effects.

1. Introduction

Underwater sound levels from pile driving are affected by site- and project-specific factors, both at the source and at longer ranges. At the source, the emitted sound levels are influenced by the dimensions and material of the driven pile, the hammer type and specifications, the water depth at the pile, the pile's depth of penetration, and the properties of the seafloor into which the pile is driven. The sound propagation spatial extent is influenced by the sound speed profile in the water column, the bathymetry of the area, and the geoacoustic properties of the seafloor. Each of these factors should be taken into consideration when conducting an impact assessment of the noise footprint associated with pile driving activities.

Noise impacts from proposed pile driving projects are often assessed based on measured noise footprints for similar activities at different locations. However, the noise-influencing factors can confound the selection of an appropriate surrogate dataset. Instead of relying on an empirical surrogate, a comprehensive numerical model can account for each of these influencing parameters and can be used to predict the sound footprint from a specific pile driving activity at a specific location.

In 2015, the Alaska Department of Transportation and Public Facilities (AKDOT&PF) funded a research project to collect empirical pile driving measurements for ferry terminal enhancements at four locations (Auke Bay, Kake, Ketchikan, and Kodiak), hereafter called "the empirical research project". This empirical data would inform AKDOT&PF about underwater sound propagation of pile driving sounds at locations in Southeast Alaska, and would be integrated into environmental impact assessments for future projects. Prior to that research project, underwater sound level data for pile driving of piles 15–40 inches in diameter (the size typical for AKDOT&PF projects) were primarily from locations in Washington State and California, with some data also coming from Southcentral Alaska. Because the available measurements varied, it was unclear how to best apply the information to other project locations. Also, the extent to which the available data were representative of the sound propagation conditions in Southeast Alaska was unknown, given differences in the geology and water column properties at the measurement locations compared to Southeast Alaska.

The measurements for the empirical research project were made from 2015-16 (Denes et al. 2016). The resulting data provided source sound level estimates and estimates of distances from the piles at which specific marine mammal impact thresholds were exceeded at each project location. The intent was that these data could then be used as surrogate information for assessments of future AKDOT&PF projects at other locations. However, the results demonstrated source sound levels varied slightly across the four project locations and the propagation distances to the marine mammal impact thresholds were quite different, highlighting the site-dependence of the underwater sound footprints. The variability of the data suggests that a numerical model that incorporates site-specific information would be useful for future impact assessments, rather than using the empirical data as a direct surrogate of the sound footprints. Therefore, a numerical modeling study was designed, the results of which we compared to the measured data to validate the model, and to better understand the factors responsible for this site variability.

These were the specific goals for the numerical modeling study:

- Validate the model estimates by comparing them to the measured data.
- Refine the estimates of the distances from the piles to the marine mammal impact thresholds that were obtained by extrapolating from the measured data.
- Interpret the model output to understand how sound propagates over distances at different sites.

This report is the outcome of the numerical modeling research project. The modeling methods are described in Section 2; the model inputs are described in detail in Section 3. Section 4 compares the modeled and measured data at the ranges and depths of acoustic recorders from the empirical research study, at each of the four project locations. Section 6 presents modeled sound level contour maps. Tables of distances to the marine mammal impact thresholds (measured and modeled) are in Section 7.

2. Methods

This study applied a two-step numerical modeling approach. First, frequency-dependent source sound levels were modeled with JASCO's Pile Driving Source Model (PDSM, Appendix A.2.1). Next, sound levels as a function of distance from the pile were computed using JASCO's FWRAM (Full-waveform Range Dependent Acoustic Model, Appendix A.2.3.2) and MONM (Marine Operations Noise Model, Appendix A.2.3.1). The models output a grid of underwater sound levels as a function of range from the pile, and of depth in the water column. The model outputs were compared with measured data from the empirical research project.

FWRAM and MONM are both frequency-dependent models that compute transmission loss by the same means, via the parabolic-equation approximation of the acoustic wave equation, accounting in the same manner for the bathymetry, the sound speed in the water column, and sediment geoacoustics. Section 3 defines the inputs used for these parameters.

FWRAM was configured for calculations along specific radials connecting the pile with the measurement locations. The FWRAM model is a time-domain acoustic propagation model that accepts as input a PDSM-generated array of point sources representing the pile. FWRAM computes synthetic pressure waveforms via Fourier synthesis, from which sound pressure level (SPL), peak level (PK), and sound exposure level (SEL) were directly obtained at ranges and depths matching those that corresponded to field measurements for comparison.

Underwater sound levels in all directions around the pile were computed with MONM because it is an efficient, frequency-domain acoustic propagation model. MONM calculations were done at the center frequencies of each 1/3-octave-band. Unlike FWRAM, MONM simulates point sources and not source arrays. Therefore, MONM simulated each pile using an equivalent point-source at the mid-point of the pile. The source level for this equivalent point-source was obtained by backpropagating the band levels from FWRAM along a single transect at ranges up to a few kilometers, and taking the mean of the backpropagated levels.

The modeled levels from MONM were maximized over depth to generate sound level contour maps, from which distances to specific marine mammal impact thresholds were determined and compared against those derived from a simple fit to the measured data. The subsections that follow give more details about each of the modeling steps.

2.1. Modeling Source Sound Levels with PDSM

A pile driving hammer imparts forces at the top of the pile, which deforms and sends vibrations along the pile wall, generating underwater sound pressure waves. This process can be simulated with numerical models. In this study, the GRLWEAP 2010 wave equation model (GRLWEAP, Pile Dynamics 2010) was used to compute the force generated by the hammer at the top of the pile.

The forcing function was input into JASCO's Pile Driving Source Model (PDSM), a physical model of pile vibration and near-field sound radiation (MacGillivray 2014), to obtain equivalent pile driving signatures consisting of a vertical array of discrete acoustic point sources (Appendix A.2.1). This vertical source-array represented the pile as an acoustic source and accounted for several parameters that describe the operation: pile type, material, size, and length and the pile driving equipment. The amplitude and phase of the point sources along the array collectively mimicked the time-frequency characteristics of the acoustic wave at the pile wall from a hammer strike (or from forced vibration in the case of vibratory driving) at the top end of the pile.

For impact pile driving, this approach accurately estimates spectral levels within the band 10–800 Hz where most of the energy from impact pile driving is concentrated. For modeling, the spectrum was extrapolated to higher frequencies using a constant decay rate of 20 dB per decade, a rate that was determined from a review of many empirical measurements at higher frequencies.

The GRLWEAP and PDSM models cannot simulate source levels for rock socket drilling. Source levels used to model drilling at Kodiak were based on the near source measurements (at 19 m rang) collected at Kodiak during the empirical research project. The maximum measured sound level was back-propagated, using transmission loss values calculated with MONM, to a surrogate source point at the mid-point of the pile.

2.2. Comparing Modeled Levels to Measurements with FWRAM

The PDSM source signatures (or drilling source levels from measurements) were input to FWRAM to compute received sound levels at the ranges and depths where acoustic measurements were made. To quantify the accuracy of the modeling approach used in this study, modeled 1/3-octave-band levels, as well as broadband SPL, SEL, and PK levels were compared to the corresponding quantities calculated from the field measurements at each site. The FWRAM model was used for this comparison because it computes the SPL and PK level metrics directly.

Results for each site are presented in the following formats:

- Plots of 1/3-octave-band levels versus frequency as modeled and measured at the closest range (nominally ~10 m range).
- Received sound levels (SEL, SPL, and PK) as a function of range at the depths where acoustic recordings were collected. Over-plotted with these data are the statistical distributions of the measured values, at the range of measurement, using a box-and-whisker format in which the box shows the 25th, 50th, and 75th percentiles, while the lower and upper whiskers show the 5th percentile and maximum measured values, respectively.

2.3. Modeling Ranges to Marine Mammal Impact Thresholds

The Level A thresholds (PK and SEL) for marine mammal injury considered in this study follow the National Marine Fisheries Service (NMFS) guidelines (NMFS 2016). Marine mammal disturbance is assessed relative to the Level B thresholds (SPL) based on the interim NMFS criteria (NMFS 2013). These thresholds are described in detail in Appendix B.

Distances to the PK thresholds for Level A harassment were computed directly from FWRAM output along the longest modeled transect. Distances to the frequency-weighted SEL, Level A, thresholds and to the SPL Level B thresholds were calculated from grids of received sound levels from MONM. Sound level contours were calculated from the sound fields output from MONM, sampled by taking the maximum value over all modeled depths above the sea floor for each location in the modeled region. The predicted distances to specific sound level thresholds were computed from these contours. Two distances relative to the source are reported for each sound level: 1) R_{max}, the maximum range to the given sound level over all azimuths, and 2) $R_{95\%}$, the range to the given sound level after the 5% farthest points were excluded (see examples in Figure 1).

The $R_{95\%}$ is used because sound field footprints are often irregular in shape. In some cases, a sound level contour might have small protrusions or anomalous isolated fringes. This is demonstrated in the image in Figure 1a. In cases such as this, where relatively few points are excluded in any given direction, R_{max} can misrepresent the area of the region exposed to such effects, and $R_{95\%}$ is considered more representative. In strongly asymmetric cases such as shown in Figure 1b, on the other hand, $R_{95\%}$ neglects to account for significant protrusions in the footprint. In such cases R_{max} might better represent the region of effect in specific directions. Cases such as this are usually associated with bathymetric features affecting propagation. The difference between R_{max} and $R_{95\%}$ depends on the source directivity and the non-uniformity of the acoustic environment.

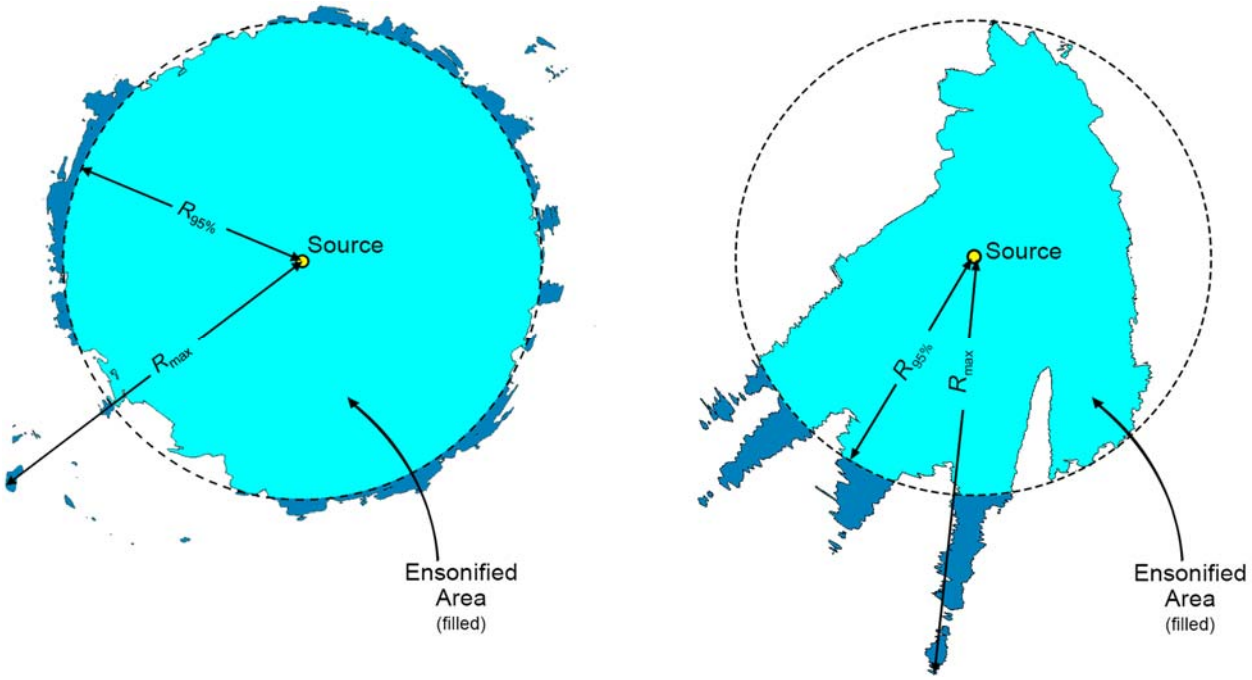

Figure 1. Sample areas ensonified to an arbitrary sound level with R_{max} and $R_{95\%}$ ranges shown for two different scenarios. (a) Largely symmetric sound level contour with small protrusions. (b) Strongly asymmetric sound level contour with long protrusions. Light blue indicates the ensonified areas bounded by $R_{95\%}$; darker blue indicates the areas outside this boundary which determine R_{max}.

2.3.1. Estimating SPL from MONM-modeled SEL results

The per-strike SEL of impact hammer pulses quantifies the sound energy, a metric related to the dose of sound received over the pulse's entire duration. The SPL of an impact hammer pulse, on the other hand, quantifies the sound intensity over a specified time interval. The time-domain model FWRAM computes both metrics directly, but the frequency-domain model MONM calculates only the SEL. Three-dimensional grids of SPLs were obtained by applying a conversion factor to the MONM-modeled per-strike SEL. For the current study, the conversion factors were calculated by computing the difference between the SEL and SPL for all ranges and depths from FWRAM, along a single radial at each site. A 125-millisecond, fixed time window was positioned to maximize the SPL over the pulse durations. The resulting SEL-to-SPL offsets were averaged in 0.5 km range bins along each modeled radial and depth; the 90th percentile over depth was selected at each range to generate a range-dependent conversion function for each site (Figure 2).

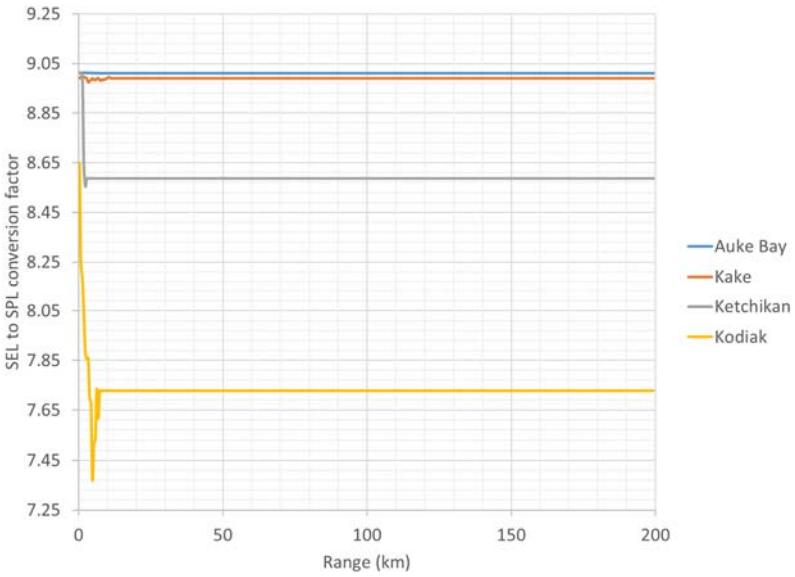

Figure 2. Range-dependent conversion factors for converting SEL-to-SPL.

2.4. Computing Total Sound Exposure Levels

MONM and FWRAM model the per-pulse SEL for impulsive sources (i.e., impact hammering) or per-second SEL for non-impulsive sources (i.e., vibratory pile driving and drilling). The NMFS criteria for assessing the potential for marine mammal injury consider the total sound exposure over the duration of an activity, so the per-pulse and per-second model outputs were accumulated for the times required to install each pile, accounting for all piles installed within the 24-hour period during which data were collected in the empirical research project. Information on the total number of strikes (impact) or the total number of seconds (vibratory and drilling) required to install piles at each site (Table 1) was used to obtain SEL_{24h}.

For impact pile driving, the SEL_{24h} was calculated by applying Equation 1:

$$SEL_{24h} = \text{per-pulse SEL} + 10 \times \log_{10} N \quad (1)$$

where N represents the total number of hammer blows for impact pile driving from the pile driving logs.

For non-impulsive sources (vibratory pile driving and drilling), the SEL_{24h} was computed by applying Equation 2:

$$\text{SEL24h} = 10 \log_{10}\left(V_{24h} 10^{SEL_V/10} + D_{24h} 10^{SEL_D/10}\right) \quad (2)$$

where SEL_V and SEL_D, correspond to the per-second SEL for vibratory pile driving or drilling, respectively, while V_{24h} and D_{24h} are the total number of seconds of operation for the vibratory hammer and the drilling, respectively, from the pile driving logs.

3. Model Parameters

3.1. Source Specifications

Model inputs parametrizing the piles, hammers, and activity details were defined to match specifications from the measurement studies at each location (Table 1). Source locations were defined to match the specific coordinates of a single pile that was measured at each location and we referenced the corresponding pile driving logs to define the number of hammer strikes and the durations for vibratory hammering and drilling for SEL calculations (as described in Section 2.4).

Table 1. Monitored and modeled pile driving activities at the four measurement locations.

Location	Kake	Auke Bay	Kodiak	Ketchikan
Dates measured	9-12 Sep 2015	10-12 Nov 2015	1-6 Mar 2016	18-21 Jul 2016
Pile driving activities monitored	Impact driving Vibratory driving Vibratory extraction	Impact driving Vibratory driving	Impact driving Vibratory driving (setting) Vibratory driving (oscillating) Rock socket drilling	Impact driving Vibratory driving
Total number of piles monitored	4*	3	8	3
Pile specifications	Diameter: 30 in* Length: 96 ft* Wall thickness: 0.5 in*	Diameter: 30 in Length: 187.8 ft Wall thickness: 0.75 in	Diameter: 24 in Length: 69 ft Wall thickness: 0.5 in	Diameter: 30 in Length: 145 ft Wall thickness: 0.5 in
Impact hammer	Delmag D19-42 Max energy: 66 kNm Piston weight: 1.82 t Blow rate: 35-52/min	Hydrohammer SC-200 Max energy: 200 kNm Piston weight: 13.6 t Blow rate: 38 blows/min	ICE Model I-36 Energy used: 91.8 kNm Piston weight: 3.6 t Stroke: 8.5 ft	Delmag D46-32 Max energy: 145.5 kNm Piston weight: 4.6 t Stroke: 10.5 ft
# of hammer strikes modeled	224	886	10	1778
Vibratory hammer	HPSI 260 Frequency: 1600 rpm Force: 890 kN Weight: 4853 kg	APE 200-6 Frequency: 0-1650 vpm Force: 2270 kN Weight: 8573 kg	ICE model 44-B with caisson clamp Frequency: 900-1800 vpm Force: 1844 kN Weight: 5647 kg	ICE model 44-B with caisson clamp Frequency: 900-1800 vpm Force: 1844 kN Weight: 5647 kg
Modeled Vibratory Duration (seconds)	1935	4544	208	19671
Drill			Power pack: APE 150 Drill bit: Numa Super Jaws Overburden Bit Air compressors (5 total, 3-4 used): IR 1070 CFM (x2), IR 1170 CFM, Sullair 1150 CFM, Sullair 950 CFM	
Modeled drilling duration (seconds)			8692	

*Two piles were extracted and two were driven with the vibratory and impact hammer. The extracted piles were battered and had a diameter of 18 in with unknown length and thickness.

3.2. Bathymetry

The bathymetry describes the water depths throughout the modeled area. For each site in this project, bathymetry data were compiled from NOAA Nav (S-57) Charts (2016). In addition, client-supplied high resolution bathymetry contours at the modeling location were also included. The final bathymetry grids had a 10 m cell size and were adjusted to represent the mean tide value (NOAA 2017) for the time interval corresponding to the pile driving activities. For the Ketchikan location, JASCO staff used an echo sounder unit on the research vessel to collect additional bathymetry data along a single transect between the two measurement locations.

3.3. Geoacoustic Profiles

Seafloor properties influence underwater sound propagation because they affect energy transmission at the water-bottom interface and through underlying sediment layers. Seabed geoacoustics in this study were based on measurements from a variety of sources such as sediment cores, seismic profiles, and analysis of grain sizes from sediment samples. The amount and type of information available for this study varied from site to site, as described in the relevant subsections.

Typically, once a plausible sediment geoacoustic profile is determined, acoustic modeling is carried out to assess the extent of the noise footprint caused by pile driving activities. However, the frequency- and range-dependent measurements of piling activities available at each site for this project allowed us to further refine the geoacoustic parameters. By iteratively performing acoustic modeling and comparing to the measurements, seabed geoacoustics were tuned to better align the modeled and measured SEL (broadband and per band), PK, and SPL.

3.3.1. Geoacoustics for Auke Bay

Field studies in the area (Alaska Department of Transportation and Public Facilities 1996) suggest that the top soil profile at Auke Bay consists of three sediment units (Table 2). Densities, sound speeds, and attenuations for silty sand, clayey silt, and sand-silt top were obtained from Hamilton (1980), while the geoacoustics for the bedrock were obtained from Brocher (2005). Attenuations in the sediment layers as well as the transition layer of fractured greenstone were obtained by iterative acoustic modeling to match the broadband SEL measured at ranges of 6.75 m, ~300 m (dipping hydrophone), and 1184 m. In addition, based on the total pile penetration during impact pile driving, we determined that the bedrock, which is formed of greenstone (NOAA/NMFS Juneau Consolidated Facility 1998), is around 27 m below the seafloor.

Table 2. Auke Bay: Geoacoustic properties. Within each depth range, each parameter varies linearly within the stated range.

Depth below seafloor (m)	Material	Density (g/cm³)	P-wave speed (m/s)	P-wave attenuation (dB/λ)	S-wave speed (m/s)	S-wave attenuation (dB/λ)
0–3.5	Silty, gravelly sand	1.77-1.77	1646-1646	1.1-1.1	160	2.10
3.5–10.5	Clayey silt	1.49-1.49	1549-1549	1.3-1.7		
10.5-27	Sand-silt	1.77-1.77	1652-1652	1.7-2.5		
27-5000	Fractured greenstone bedrock	1.77-2.50	1700-6600	2.5-0.6		
> 5000	Greenstone bedrock	2.50	6600	0.12		

3.3.2. Geoacoustics for Kake

Field studies in the area (Dames & Moore 1973) suggest that the soil profile at Kake consists of a top layer of alluvium (~3 m thick) on top of till (at least 5 m thick). The bedrock was identified as metamorphosed basalt and graywacke, with evidence of fracturing. Densities, sound speeds, and attenuations for the alluvium (Table 3) correspond to sand sediment obtained from Jensen et al. (2011). Geoacoustics for till at 3 m depth were set to match the properties of the glacial till (Quijano et al. 2016) model, while properties for the bedrock substrate were selected to match those for sandstone-basalt (Briggs and Fischer 1992). The thickness of the till layer and the attenuations for alluvium and till were adjusted to match the measured SEL at 10 m, 60-160 m (dipping hydrophone), and 1098 m.

Table 3. Kake: Geoacoustic properties. Within each depth range, each parameter varies linearly within the stated range.

Depth below seafloor (m)	Material	Density (g/cm³)	P-wave speed (m/s)	P-wave attenuation (dB/λ)	S-wave speed (m/s)	S-wave attenuation (dB/λ)
0–3.0	Alluvium	1.30-1.90	1510-1650	1.2-1.2	153	2.50
3.0–50.0	Till	1.47-2.10	1521-2000	1.6-1.6		
> 50.0	Bedrock (metamorphosed basalt and graywacke)	2.2	2940	0.09		

3.3.3. Geoacoustics for Ketchikan

Field studies in the area (Dames & Moore 1973) suggest that the soil profile at Ketchikan consists of a sand layer (22 m thick) on top of phyllite and schist bedrock. Analysis of sand samples collected at the modeling location indicates grain sizes predominantly range between 0.15 mm-2 mm. A sediment grain-shearing model (Buckingham 2005) with an input grain size of 1 mm was used to estimate the density, compressional-wave speed, shear-wave speed, and compressional-wave attenuation for the sand layer (Table 4). Geoacoustics corresponding to the bedrock were obtained from King et al. (2008). The attenuation for the sand layer was adjusted to match the measured SEL at 16 m, 80-270 m (dipping hydrophone), and 947 m.

Table 4. Ketchikan: Geoacoustic properties. Within each depth range, each parameter varies linearly within the stated range.

Depth below seafloor (m)	Material	Density (g/cm³)	P-wave speed (m/s)	P-wave attenuation (dB/λ)	S-wave speed (m/s)	S-wave attenuation (dB/λ)
0–22.0	Sand	2.09-2.09	1774-2292	0.32-0.95	255	3.653
> 22.0	Bedrock (phyllite and schist)	2.70	4850	0.12		

3.3.4. Geoacoustics for Kodiak

Field studies in the area (R&M Consultants 2013) suggest that the soil profile at Kodiak consists of a top sediment layer (~6 m thick)above phyllitic greywacke bedrock. In addition, because drilling-assisted pile driving was required to install the piles into the bedrock, the bedrock is likely intact as opposed to fractured. A notch in the measured band levels around 110 Hz suggests that the top sediment layer at Kodiak allows for high energy transmission due to pile driving into the bedrock, which is likely to strongly support shear wave propagation (see Appendix C). Based on these assumptions, geocaoustics for Kodiak used in this report consist of a top layer of glacial till, followed by a thin layer of coarse sand on top of bedrock (Table 5). As discussed in Appendix C, this geoacoustic profile supports conservative estimation of the acoustic propagation from down-the-hole (DTH) drilling and impact/vibratory pile driving. To more accurately estimate the actual levels that were measured at Kodiak, the modeling also considered shear sound speed of 1300 m/s in the bedrock, which results in smaller noise footprints.

Table 5. Kodiak: Geoacoustic properties. Within each depth range, each parameter varies linearly within the stated range.

Depth below seafloor (m)	Material	Density (g/cm^3)	P-wave speed (m/s)	P-wave attenuation (dB/λ)	S-wave speed (m/s)	S-wave attenuation (dB/λ)
0–6.0	Glacial till	1.4-1.4	1520-1520	0.7-0.7	100	2.4
6.0-6.17	Coarse sand	2.06-2.06	1845-1845	0.8-0.8		
> 6.17	Bedrock	2.1	2940	0.2		

4. Modeled Source Levels

Figure 3 is a plot of the forcing functions from GRLWEAP that were input to PDSM to generate the array of source monopoles for FWRAM. For vibratory pile driving, the GRLWEAP forces in Figure 3(right), are periodic with their fundamental frequency determined by the pile driver. Since the PDSM is a linear model, the resulting source levels were mostly concentrated at the single frequency band that includes the hammer's fundamental frequency. While this method is correct in principle, field measurements for vibratory pile driving often exhibit energy at multiple harmonics of the hammer's fundamental frequency. To incorporate this effect into the model, the amplitude of the vibratory forces in Figure 3(right) was modified to introduce non-linearities, which results in the spread of some of the vibratory energy to higher frequencies (Appendix A.2.2).

Figure 4 is a plot of the point-source equivalent source sound levels, in 1/3-octave-bands, that were input to MONM for impact and vibratory pile driving at each site. Source levels input to MONM for drilling at Kodiak are plotted in Figure 5.

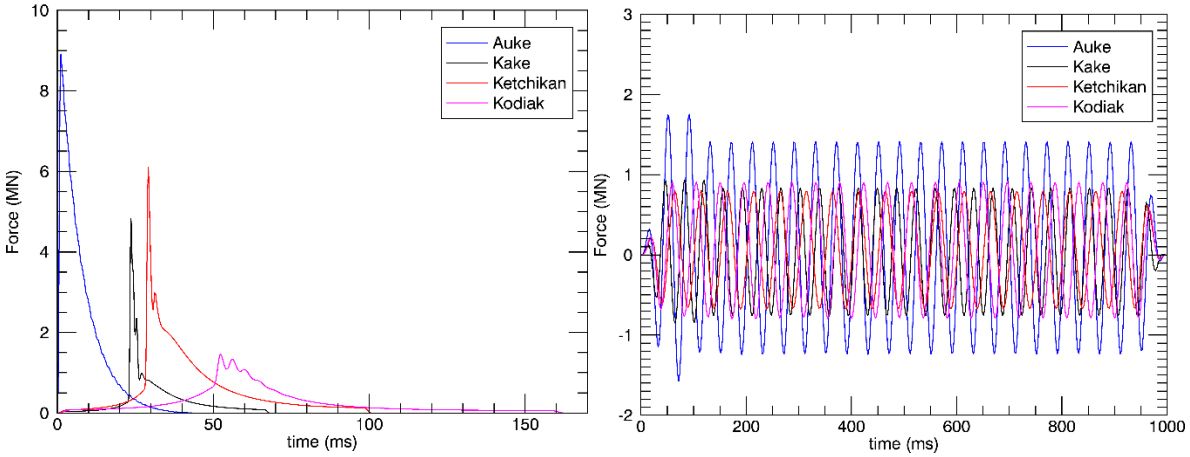

Figure 3. Force at the top of the pile corresponding to (left) impact and (right) vibratory pile driving at the four locations considered in this study. The forcing functions were computed using the GRLWEAP 2010 wave equation model for the hammer and pile dimensions described in Table 1.

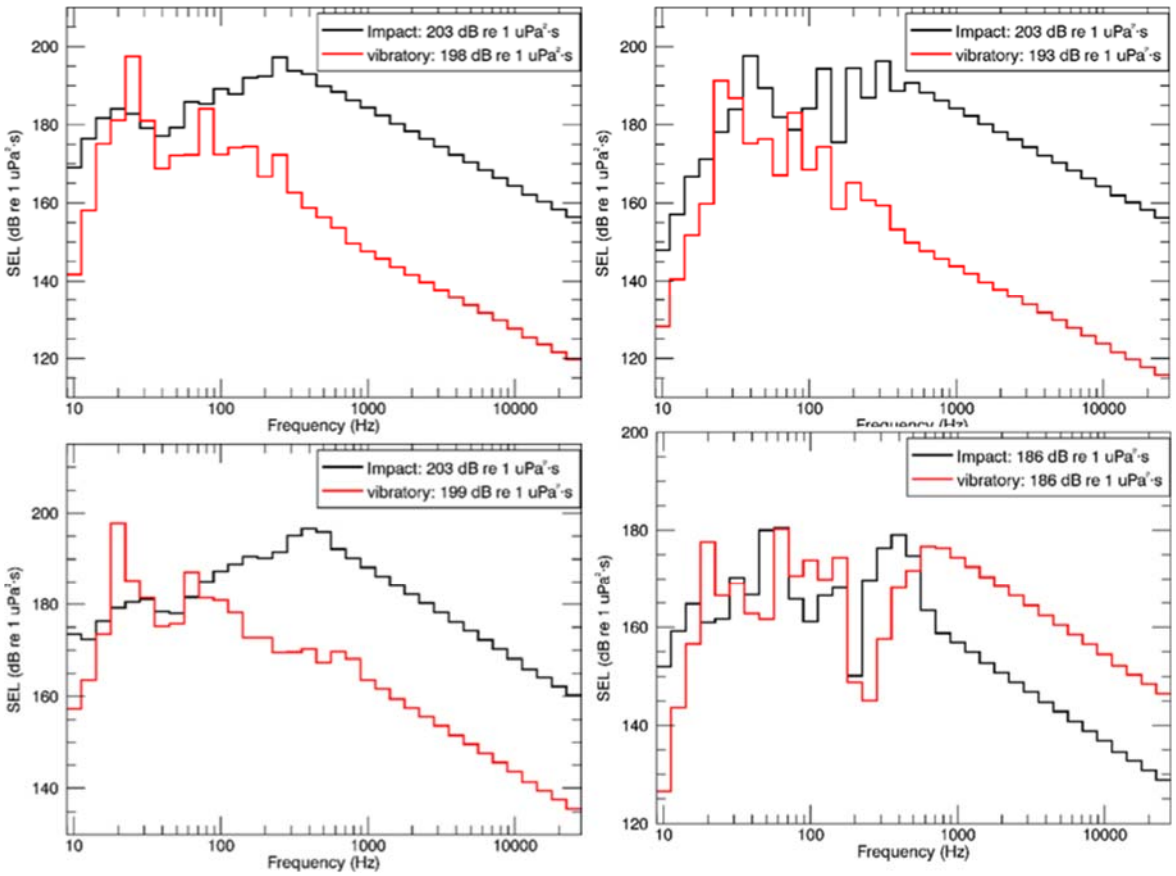

Figure 4. Source levels in 1/3-octave-bands used to model impact and vibratory pile driving at (top left) Auke Bay, (top right) Kake, (bottom left) Ketchikan, and (bottom right) Kodiak.

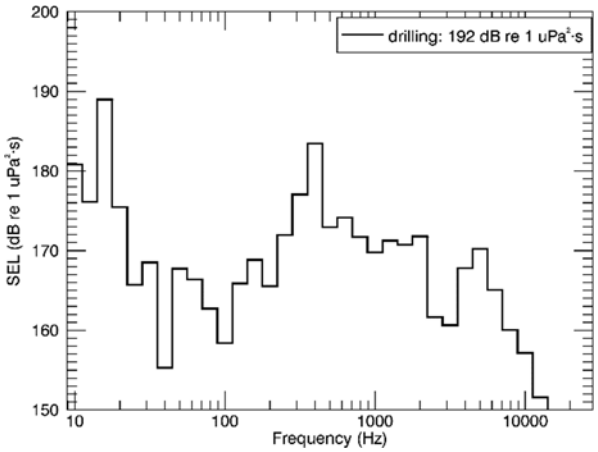

Figure 5 Source levels in 1/3-octave-bands used to model drilling at Kodiak.

5. Comparing Modeled and Measured Levels

In this section, the model results are compared with measured data from each site. Plots of near-source sound levels in 1/3-octave-bands illustrate the accuracy with which PDSM replicates the spectral dependency of the source functions for impact and vibratory pile driving. Plots of broadband sound levels as a function of range illustrate the similarities between the FWRAM propagation model estimations compared to the measured data.

5.1. Auke Bay

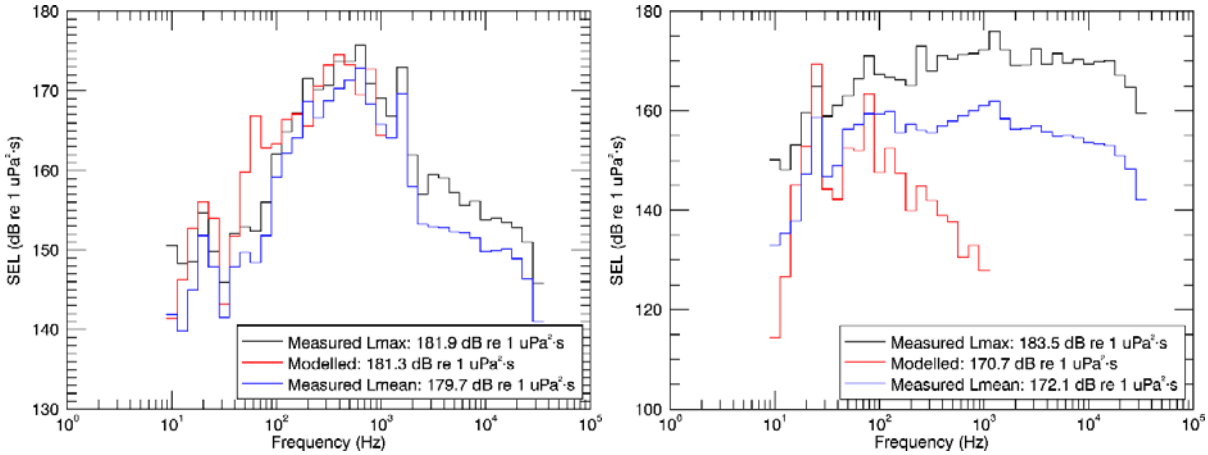

Figure 6. Auke Bay: Modeled band labels for (left) impact and (right) vibratory pile driving compared to measured band levels (maximum and mean) at the closest measurement range of 7m (Denes et al. 2016).

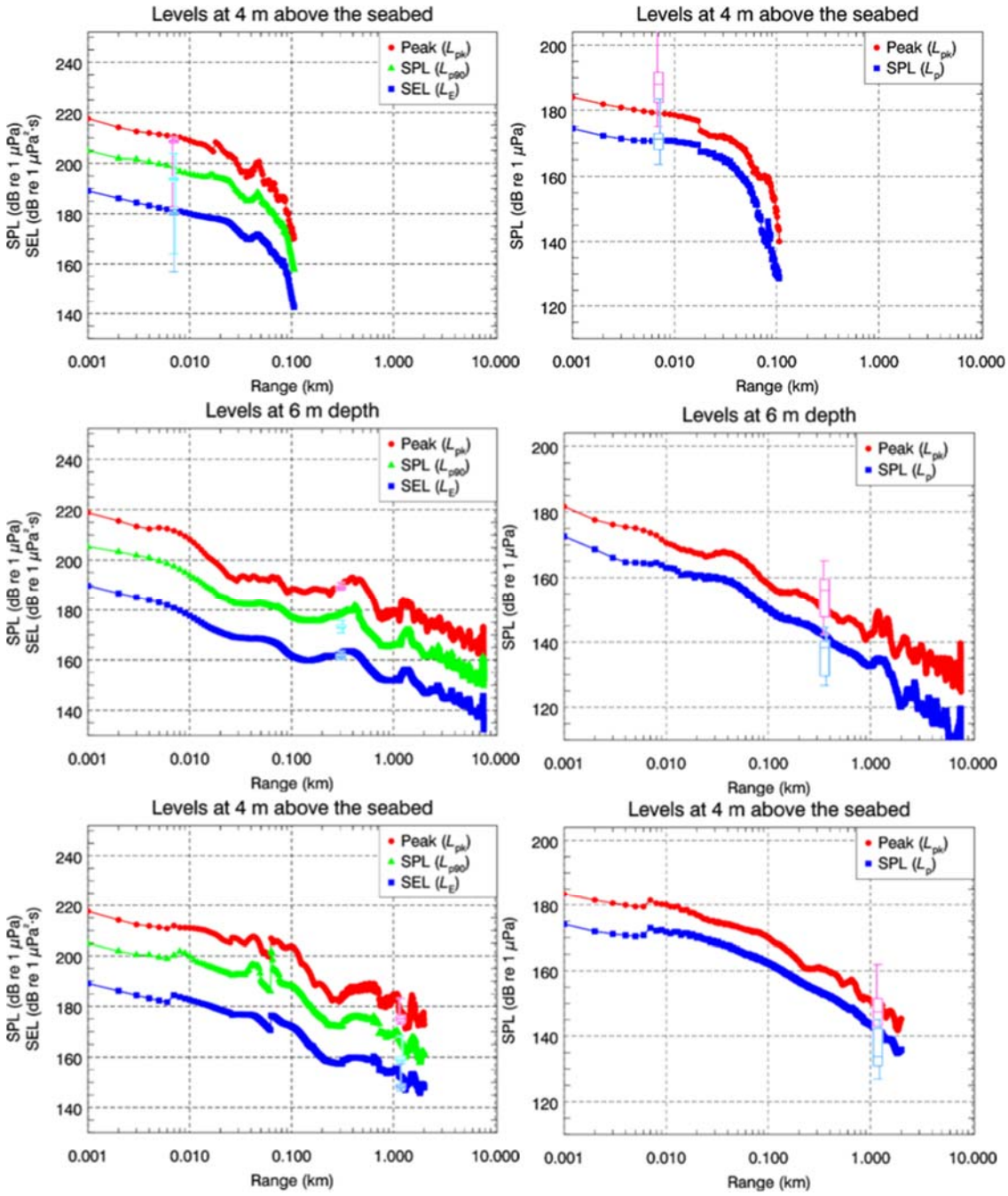

Figure 7. Auke Bay: Comparison of modeled and measured SEL, SPL, and PK levels for (left column) impact and (right column) vibratory pile driving. The ranges for the measurements are 7 m (top row), 296-306 m for impact and 358-360 m for vibratory pile driving (middle row), and 1184 m (bottom row). The receiver depths for the data correspond to the hydrophone depth at each range. The measured data are presented using a box-and-whisker format in light blue, indigo, and magenta for SEL, SPL, and PK levels, respectively.

5.2. Kake

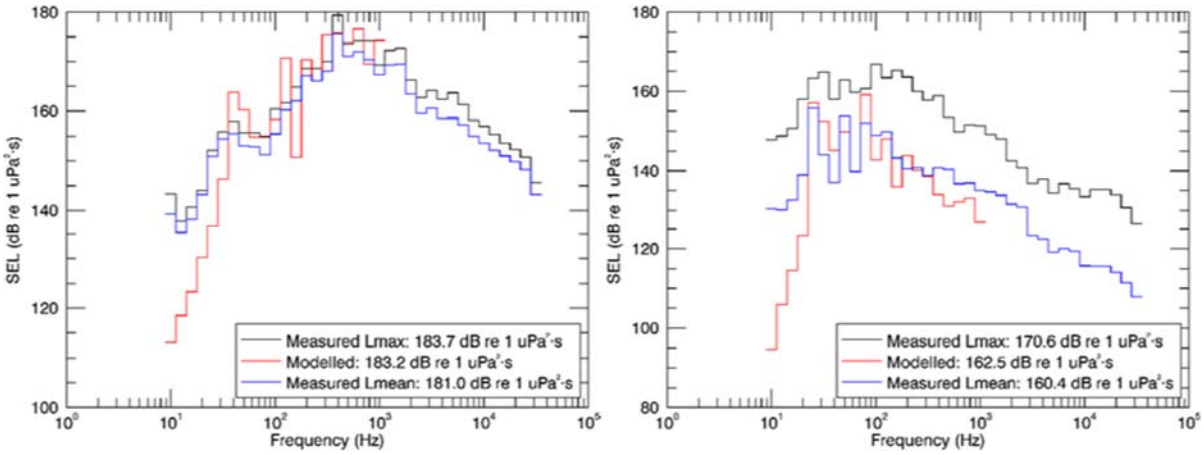

Figure 8. Kake: Modeled band labels for (left) impact and (right) vibratory pile driving compared to measured band levels (maximum and mean) at the closest measurement range of 9.5m (Denes et al. 2016).

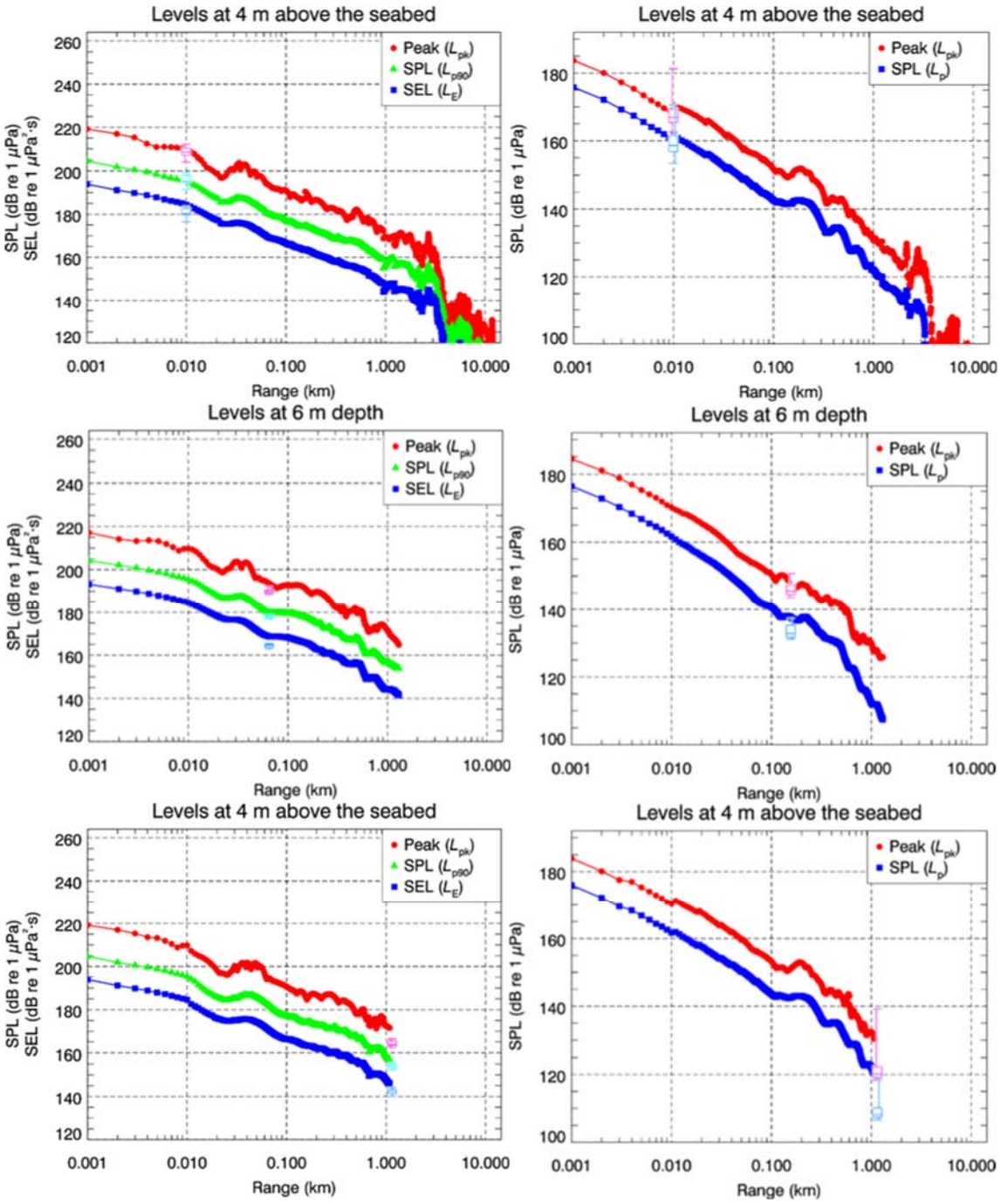

Figure 9. Kake: Comparison of modeled and measured SEL, SPL, and PK levels (left column) impact and (right column) vibratory pile driving. The ranges for the measurements are 9.5 m (top row), 61-69 m for impact and 146-166 m for vibratory pile driving (middle row), and 1098 m (bottom row). The receiver depths for the data correspond to the hydrophone depth at each range. The measured data are presented using a box-and-whisker format in light blue, indigo, and magenta for SEL, SPL, and PK levels, respectively.

5.3. Ketchikan

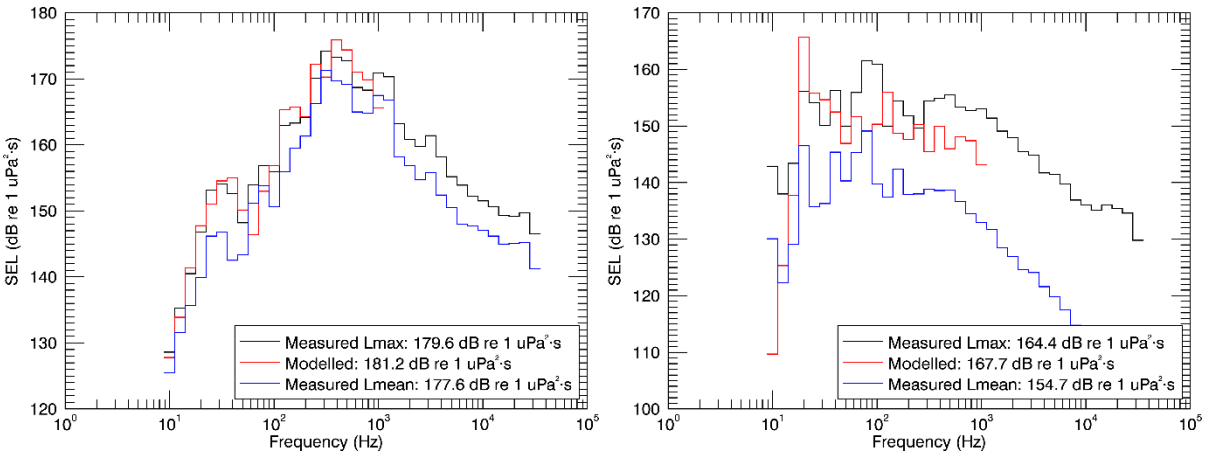

Figure 10. Ketchikan: Modeled band labels for (left) impact and (right) vibratory pile driving compared to measured band levels (maximum and mean) at the closest measurement range of 17.3 m (Denes et al. 2016).

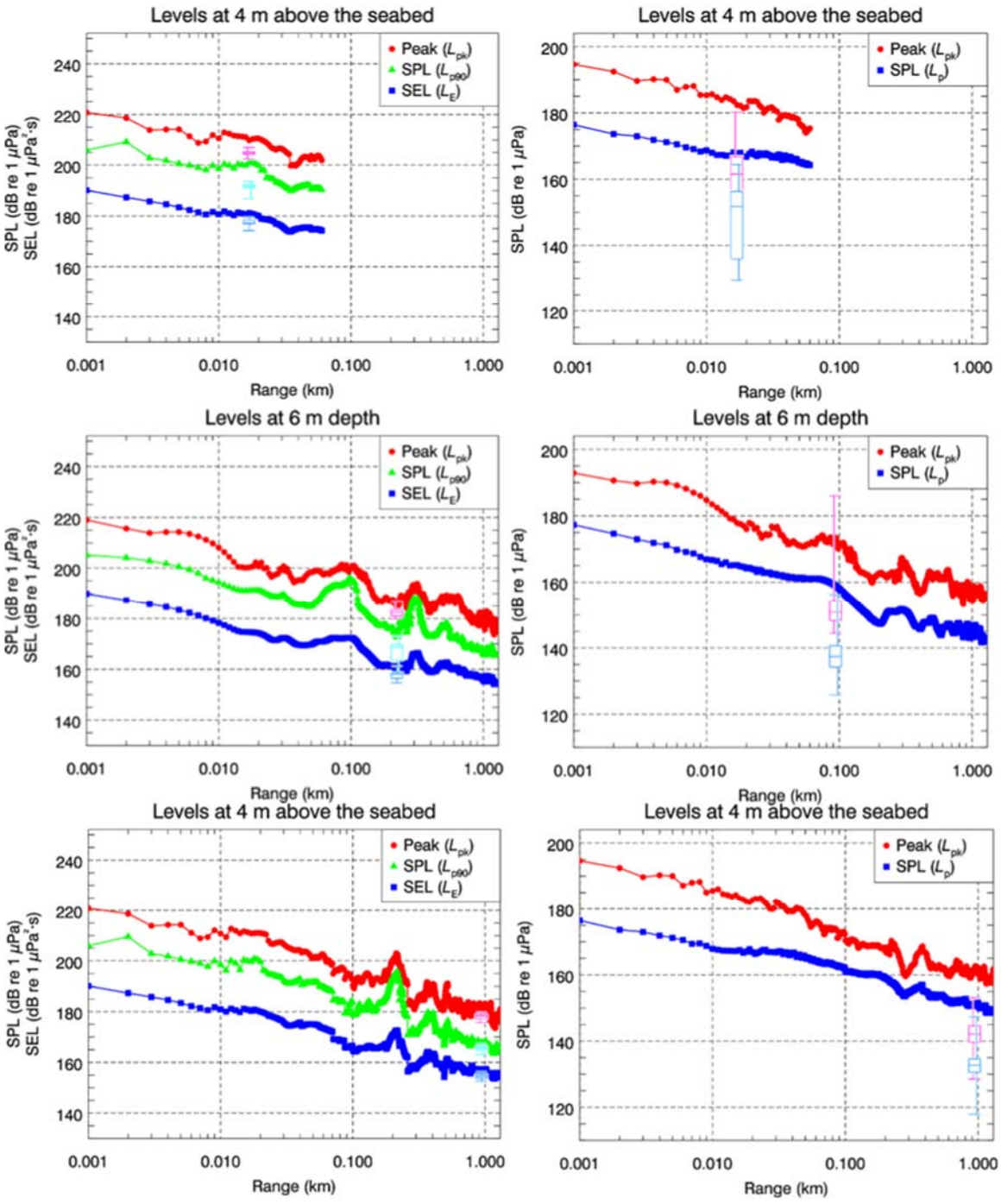

Figure 11. Ketchikan: Comparison of modeled and measured SEL, SPL, and PK levels for (left column) impact and (right column) vibratory pile driving. The ranges for the measurements are 17.3 m (top row), 120-298 m for impact and 66-110 m for vibratory pile driving (middle row), and 948 m (bottom row). The receiver depths for the data correspond to the hydrophone depth at each range. The measured data are presented using a box-and-whisker format in light blue, indigo, and magenta for SEL, SPL, and PK levels, respectively.

5.4. Kodiak

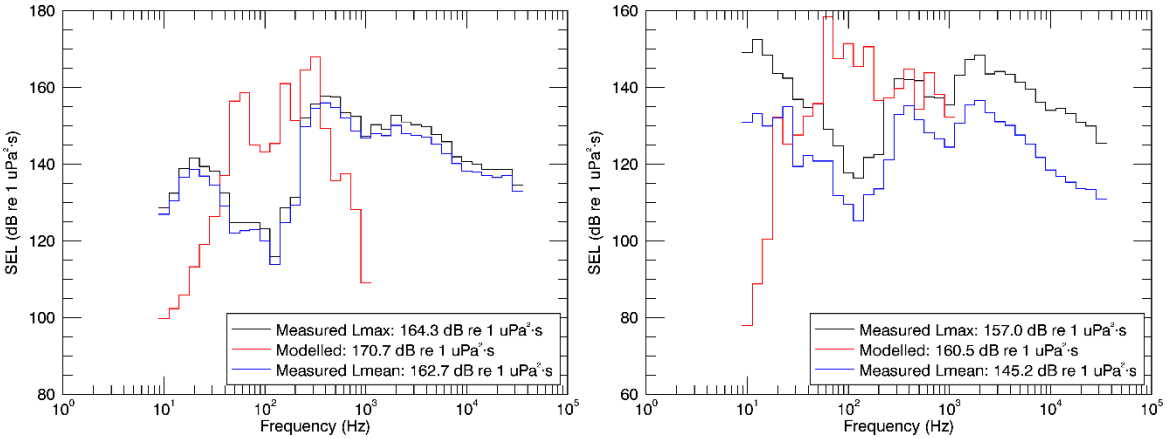

Figure 12. Kodiak: Modeled band labels for (left) impact and (right) vibratory pile driving compared to measured band levels (maximum and mean) at the closest measurement range of 16 m(Denes et al. 2016).

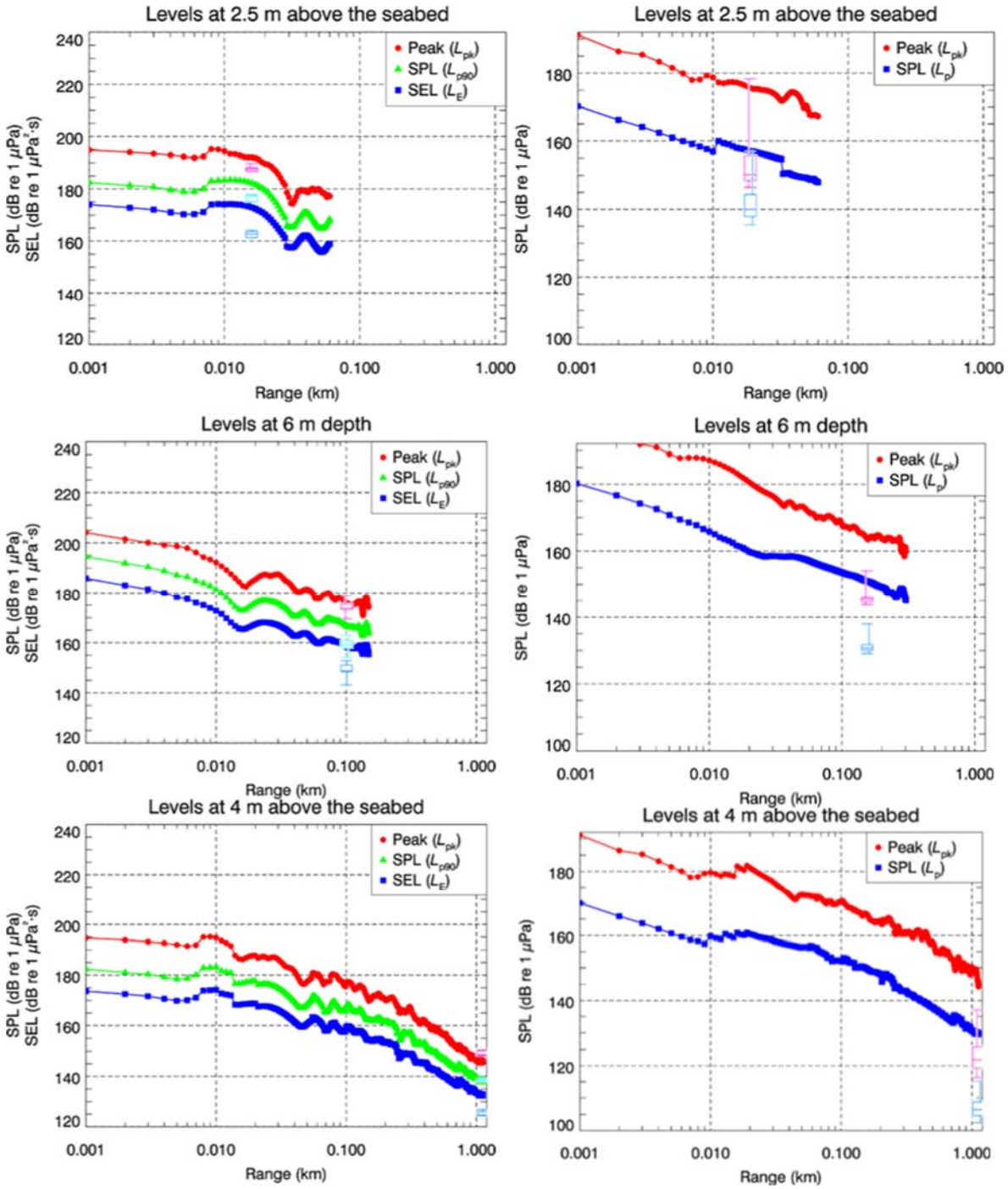

Figure 13. Kodiak Comparison of modeled and measured SEL, SPL, and PK levels (left column) impact and (right column) vibratory pile driving. The ranges for the measurements are 16 m (top row), 69-177 m for impact and 150-161 m for vibratory pile driving (middle row), and 1122 m (bottom row). The receiver depths for the data correspond to the hydrophone depth at each range. The measured data are presented using a box-and-whisker format in light blue, indigo, and magenta for SEL, SPL, and PK levels, respectively.

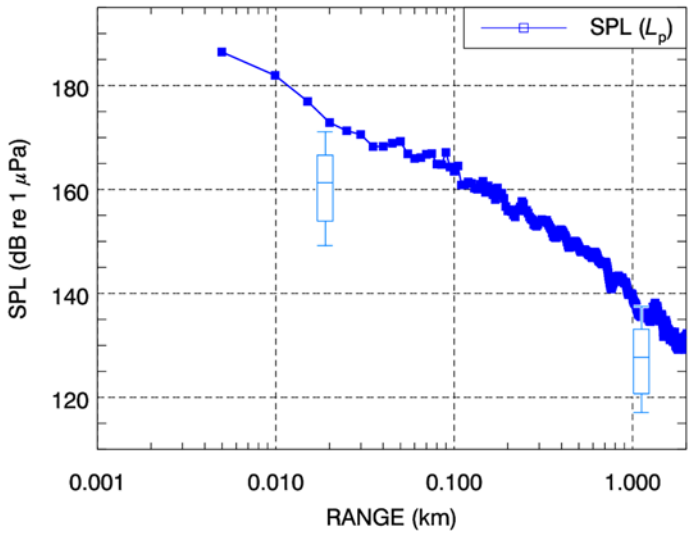

Figure 14. Kodiak: Comparison of modeled and measured SEL for drilling.

6. Sound Level Contours

This section describes the spatial distribution of the sound fields modeled with MONM for each site. Colored shade-plots of SPL range-depth slices, along a radial from the pile to the farthest measurement range, depict the distribution of the sound levels throughout the water column and the interaction between sound and the seafloor.

Contour maps show the planar distribution of the levels maximized over depth in the water. Contours for the marine mammal impact thresholds for impact and vibratory pile driving are provided for each site, and for drilling at Kodiak. Solid-filled contours show the spatial extent of the sound levels that exceed the SEL thresholds for marine mammal injury, by functional hearing group. A patterned contour depicts the area ensonified above the broadband SPL threshold for behavioral disturbance. Circular curves show the modeled R_{max} and $R_{95\%}$ boundaries (the values for which are given Section 7) for the behavioral disturbance threshold; the mean and 90th percentile distances to this threshold from the empirical data fits are shown for comparison, as is distance obtained using the Practical Spreading Loss Model assumption (that is, assuming that sound decays with range, R, at a rate of 15logR) and the mean measured source level for each pile. These circles are visual constructs of the threshold distances but do not depict true acoustic footprints, in that they are not truncated where sound is obstructed by land.

6.1. Auke Bay

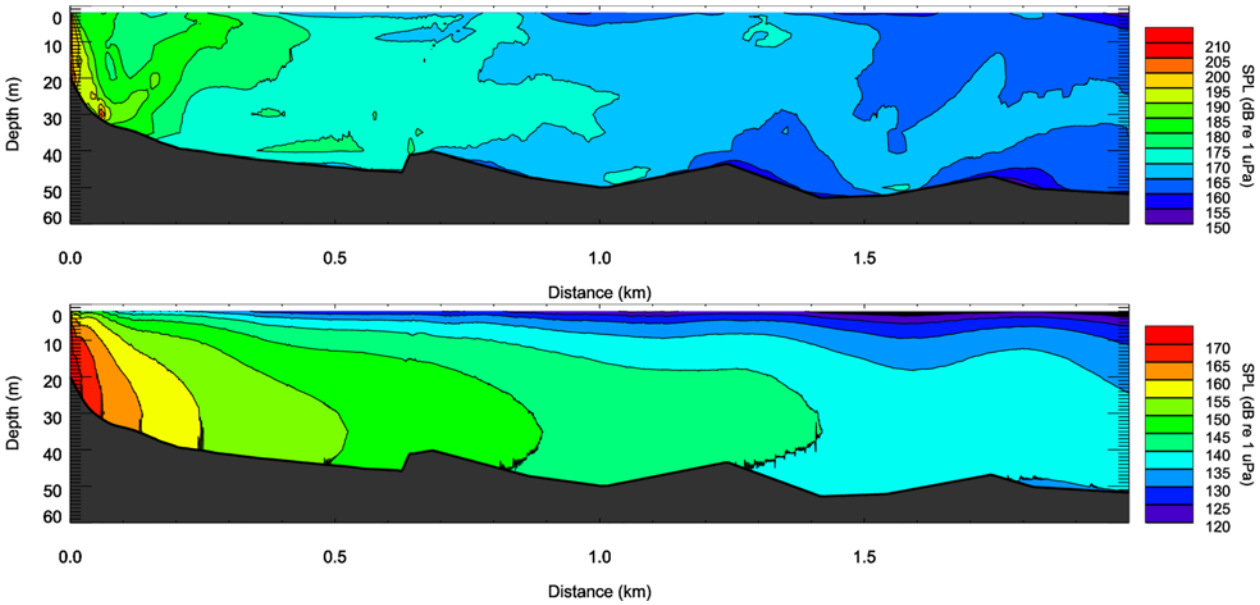

Figure 15. Auke Bay: Spatial dependency of the modeled SPL for (top) impact and (bottom) vibratory pile driving, along a transect from the pile in the direction of the furthest measurement point. The bathymetry along the selected transect is shown with black shading.

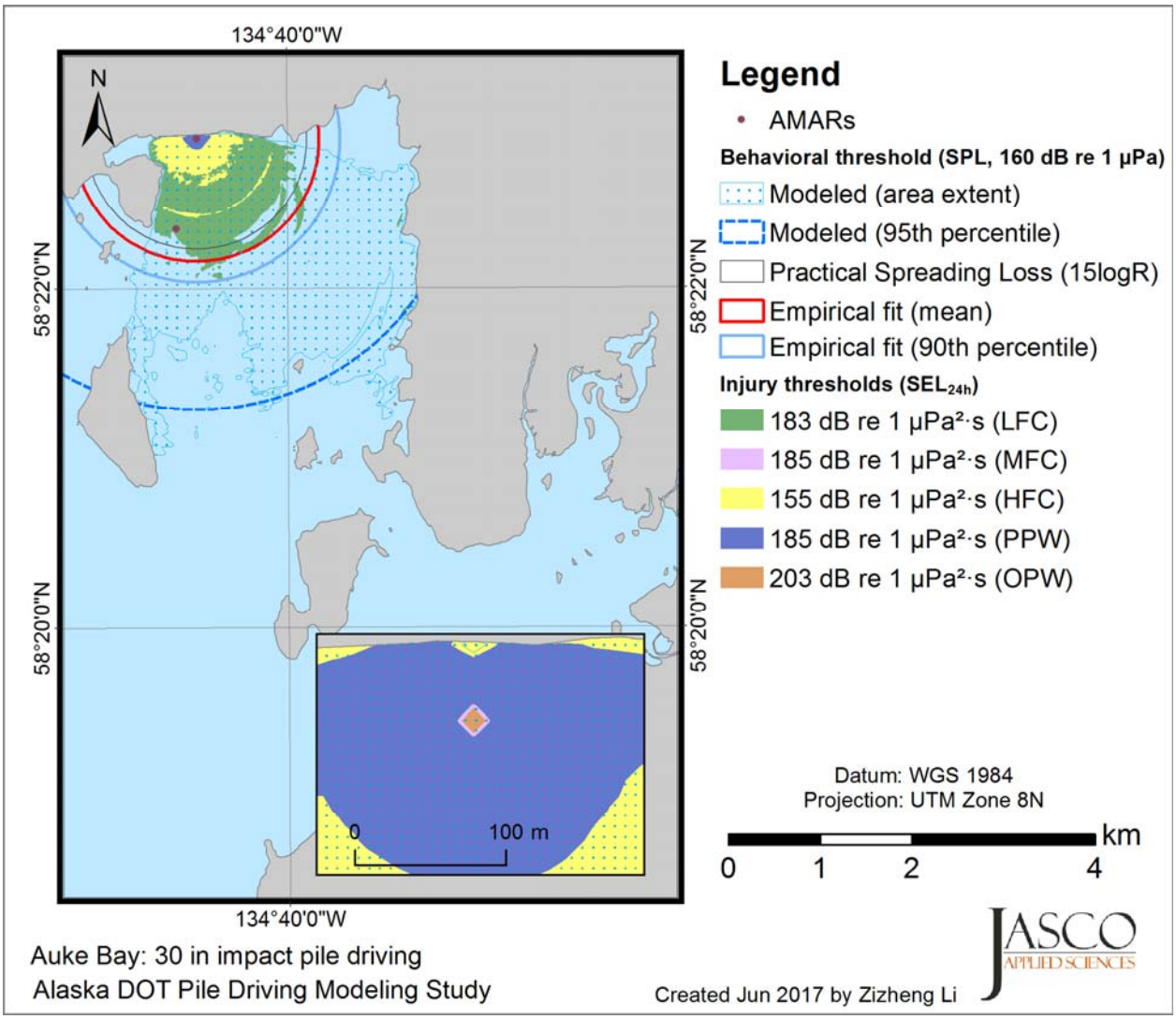

Figure 16. Auke Bay: Contours to thresholds for marine mammal injury and behavioral disturbance from impulsive sources for impact pile driving. The inset shows a close-up of sound fields around the pile location. Also shown are circles of radii corresponding to the mean and 90th percentile behavioral impact threshold distances derived from the empirical research project and from the $R_{95\%}$ modeled distance as well as from a Practical Spreading Loss model assumption and the mean measured source level. Solid circles marked AMARs are the measurement locations from the empirical research project..

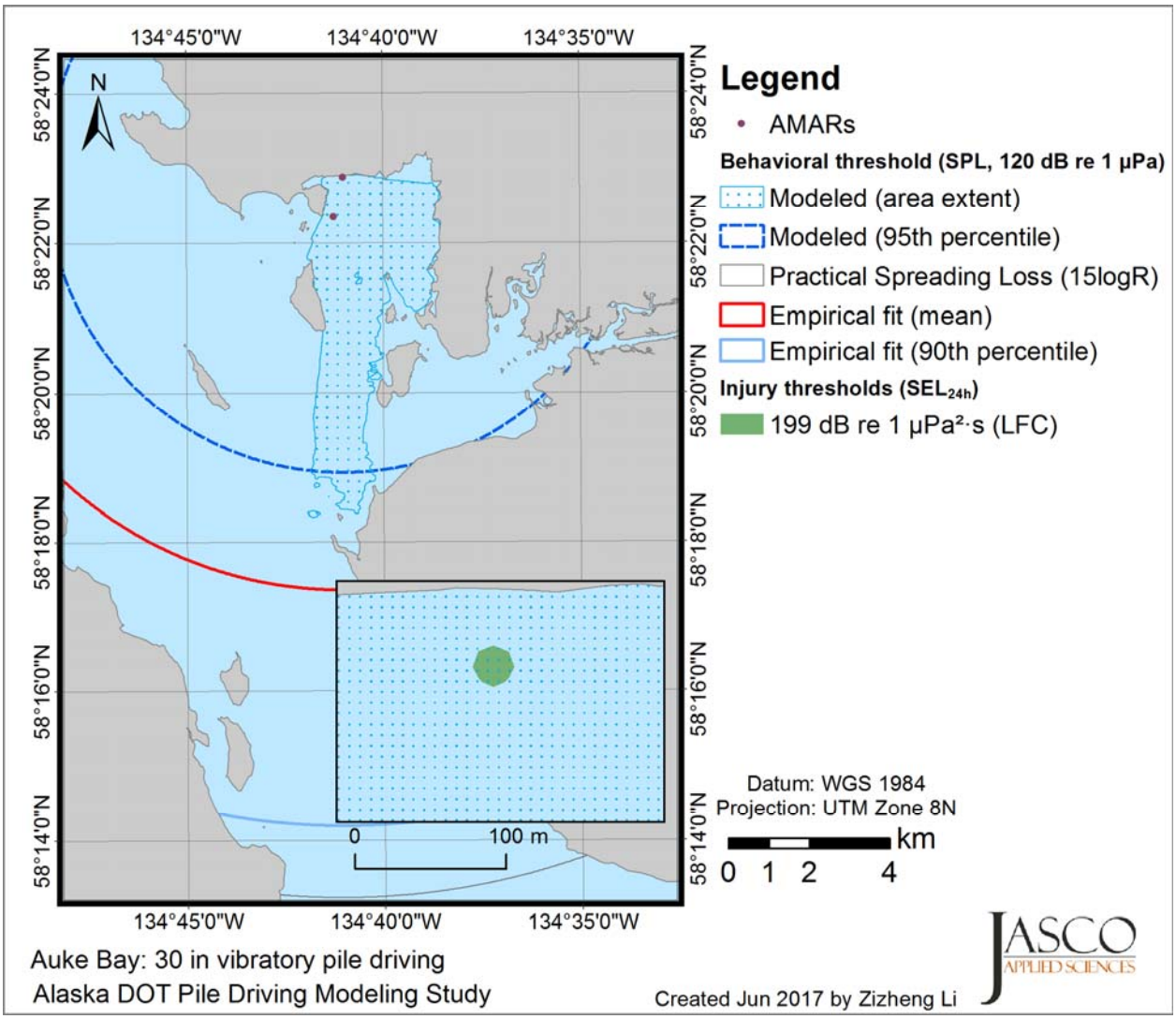

Figure 17. Auke Bay: Contours to thresholds for marine mammal injury (where exceeded) and behavioral disturbance from non-impulsive sources for vibratory pile driving. The inset shows a close-up of sound fields around the pile location. Also shown are circles of radii corresponding to the mean and 90th percentile behavioral impact threshold distances derived from the empirical research project and from the $R_{95\%}$ modeled distance as well as from a Practical Spreading Loss model assumption and the mean measured source level. Solid circles marked AMARs are the measurement locations from the empirical research project..

6.2. Kake

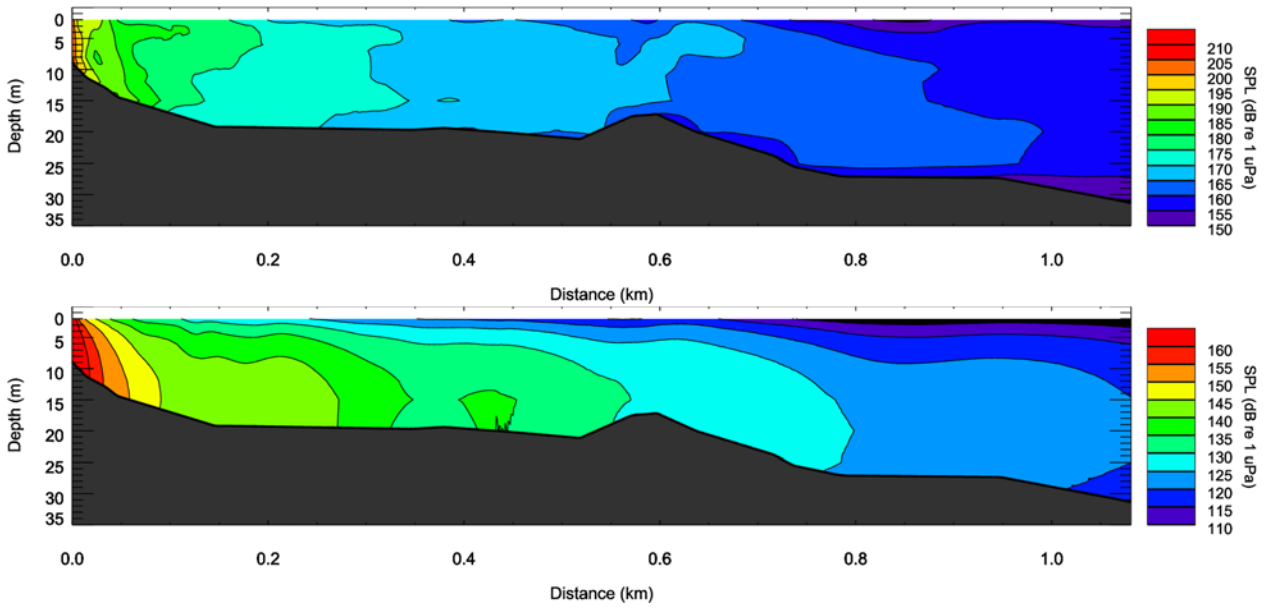

Figure 18. Kake: Spatial dependency of the modeled SPL for (top) impact and (bottom) vibratory pile driving, along a transect from the pile in the direction of the furthest measurement point. The bathymetry along the selected transect is shown with black shading.

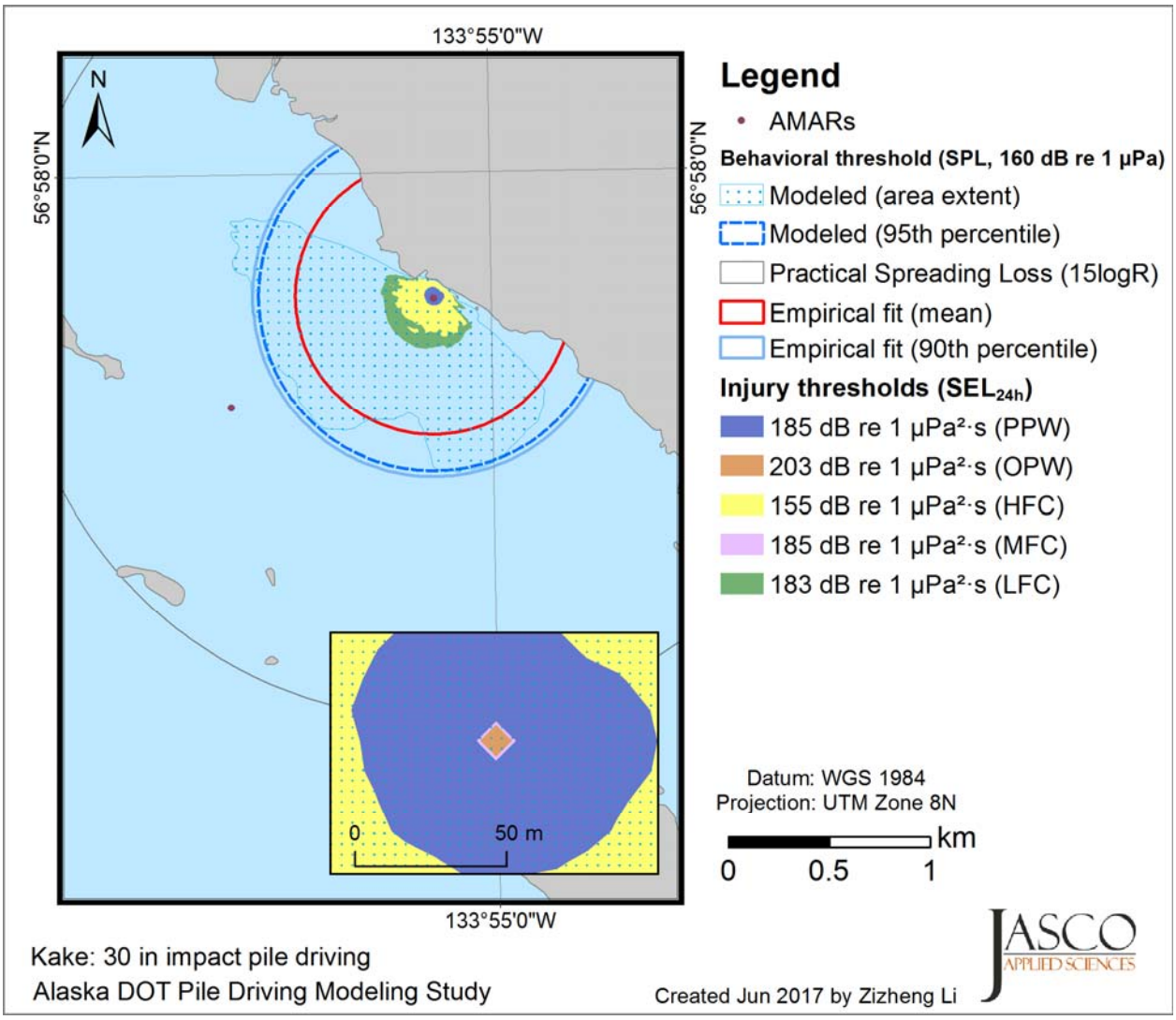

Figure 19. Kake: Contours to thresholds for marine mammal injury and behavioral disturbance from impulsive sources for impact pile driving. The inset shows a close-up of sound fields around the pile location. Also shown are circles of radii corresponding to the mean and 90th percentile behavioral impact threshold distances derived from the empirical research project and from the $R_{95\%}$ modeled distance as well as from a Practical Spreading Loss model assumption and the mean measured source level. Solid circles marked AMARs are the measurement locations from the empirical research project..

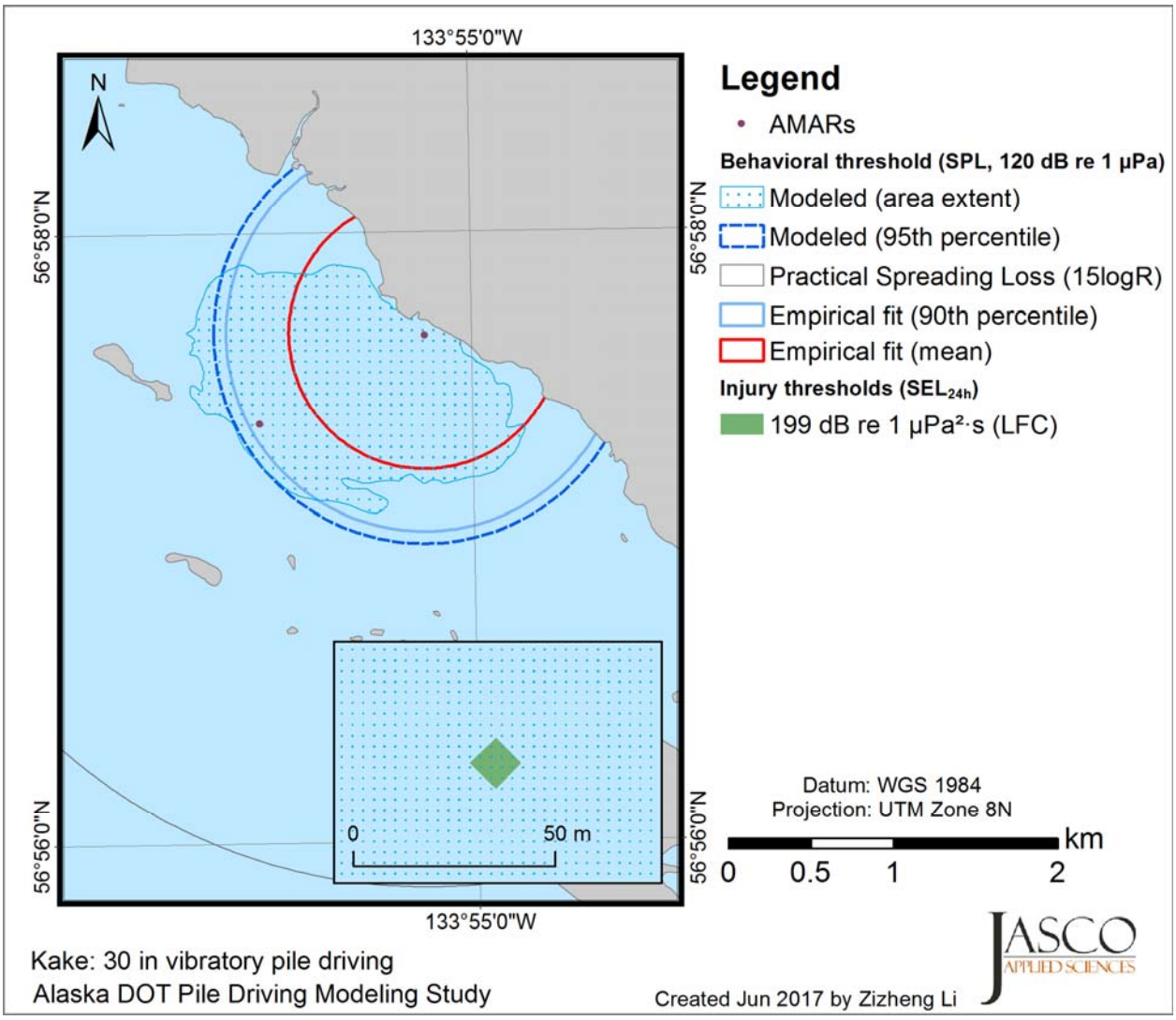

Figure 20. Kake: Contours to thresholds for marine mammal injury (where exceeded) and behavioral disturbance from non-impulsive sources for vibratory pile driving. The inset shows a close-up of sound fields around the pile location. Also shown are circles of radii corresponding to the mean and 90th percentile behavioral impact threshold distances derived from the empirical research project and from the $R_{95\%}$ modeled distance as well as from a Practical Spreading Loss model assumption and the mean measured source level. Solid circles marked AMARs are the measurement locations from the empirical research project..

6.3. Ketchikan

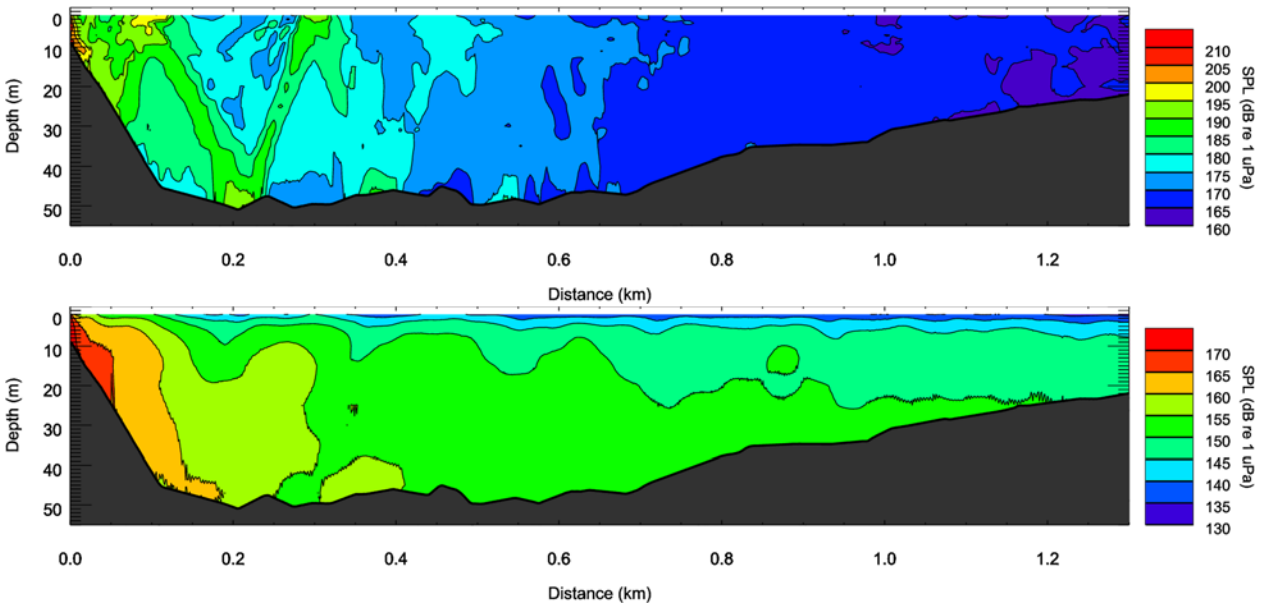

Figure 21. Ketchikan: Spatial dependency of the modeled SPL for (top) impact and (bottom) vibratory pile driving, along a transect from the pile in the direction of the furthest measurement point. The bathymetry along the selected transect is shown with black shading.

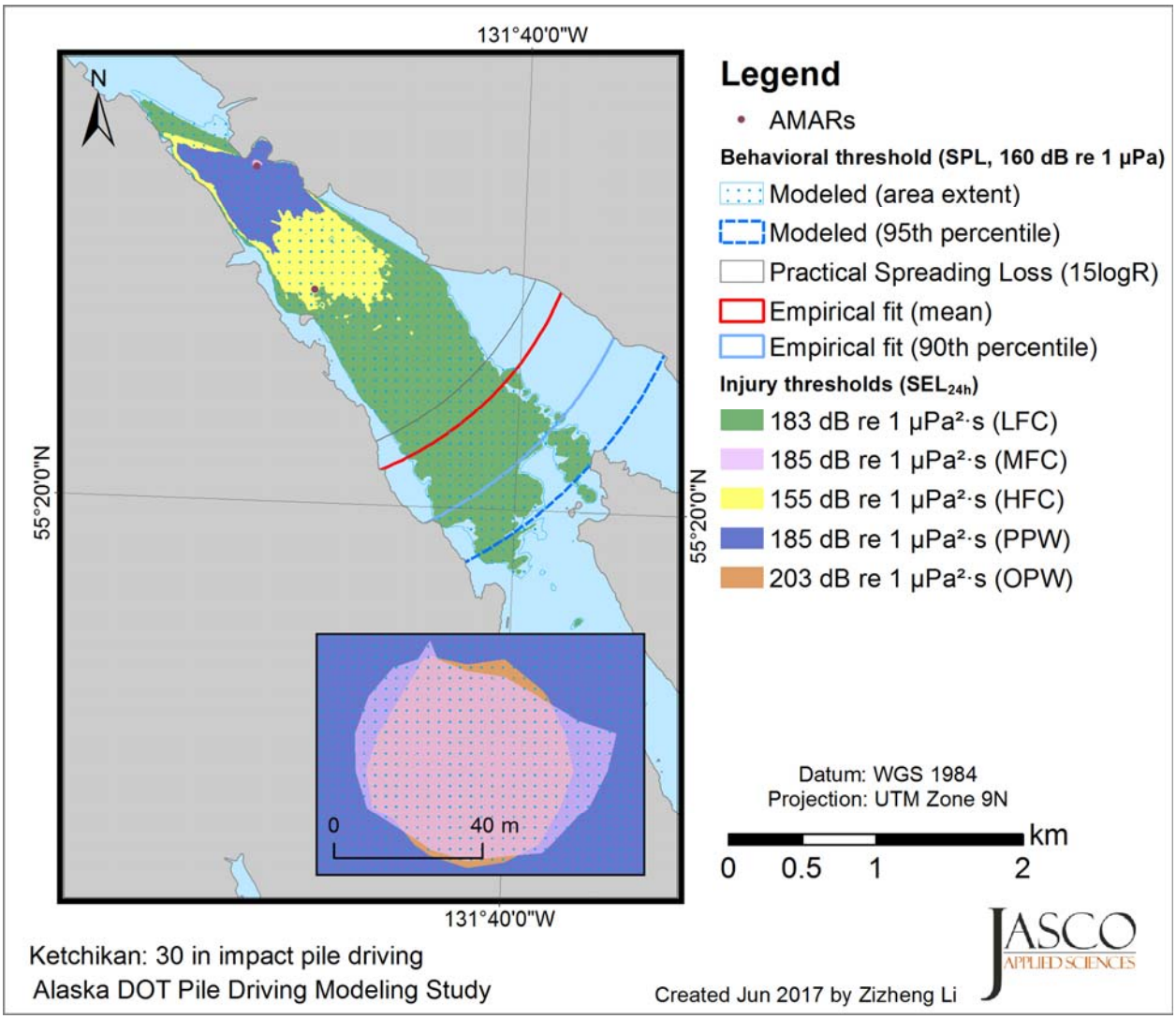

Figure 22. Ketchikan: Contours to thresholds for marine mammal injury and behavioral disturbance from impulsive sources for impact pile driving. The inset shows a close-up of sound fields around the pile location. Also shown are circles of radii corresponding to the mean and 90th percentile behavioral impact threshold distances derived from the empirical research project and from the $R_{95\%}$ modeled distance as well as from a Practical Spreading Loss model assumption and the mean measured source level. Solid circles marked AMARs are the measurement locations from the empirical research project..

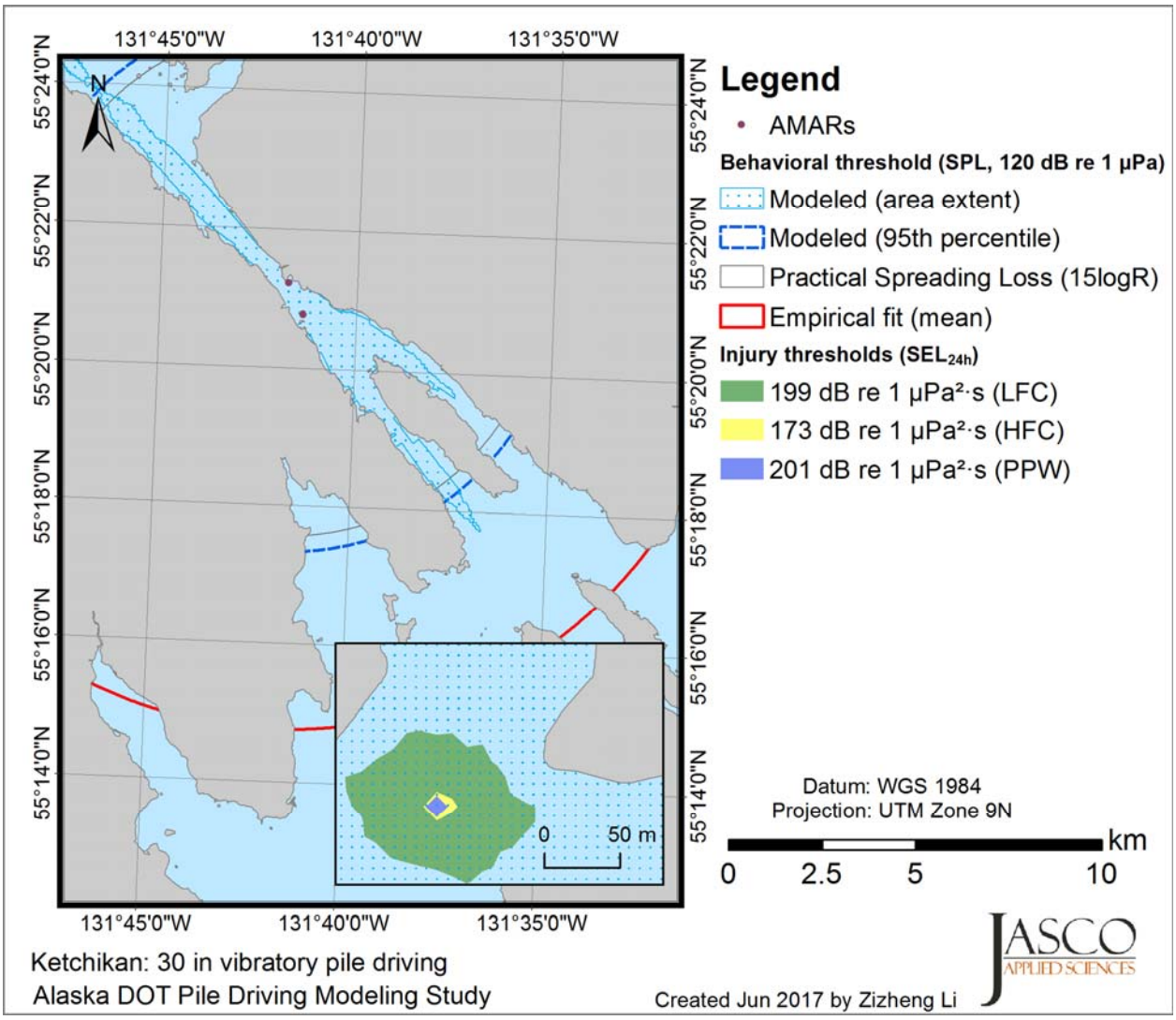

Figure 23. Ketchikan: Contours to thresholds for marine mammal injury (where exceeded) and behavioral disturbance from non-impulsive sources for vibratory pile driving. The inset shows a close-up of sound fields around the pile location. Also shown are circles of radii corresponding to the mean and 90th percentile behavioral impact threshold distances derived from the empirical research project and from the $R_{95\%}$ modeled distance as well as from a Practical Spreading Loss model assumption and the mean measured source level. Solid circles marked AMARs are the measurement locations from the empirical research project..

6.4. Kodiak

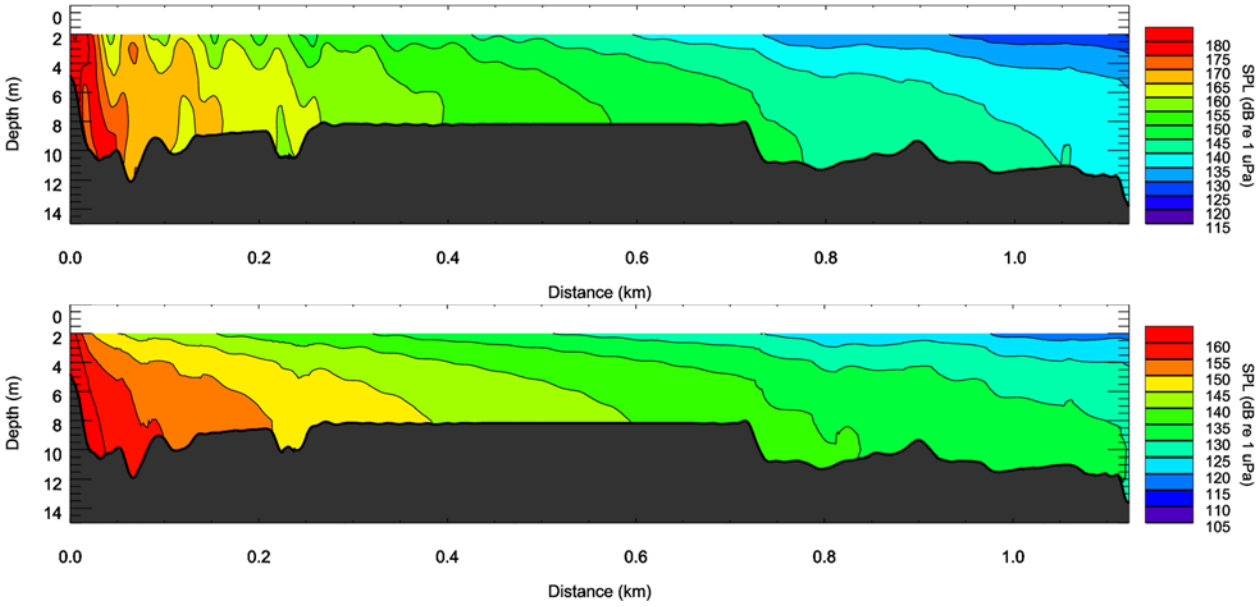

Figure 24. Kodiak: Spatial dependency of the modeled SPL for (top) impact and (bottom) vibratory pile driving, along a transect from the pile in the direction of the furthest measurement point. The bathymetry along the selected transect is shown with black shading.

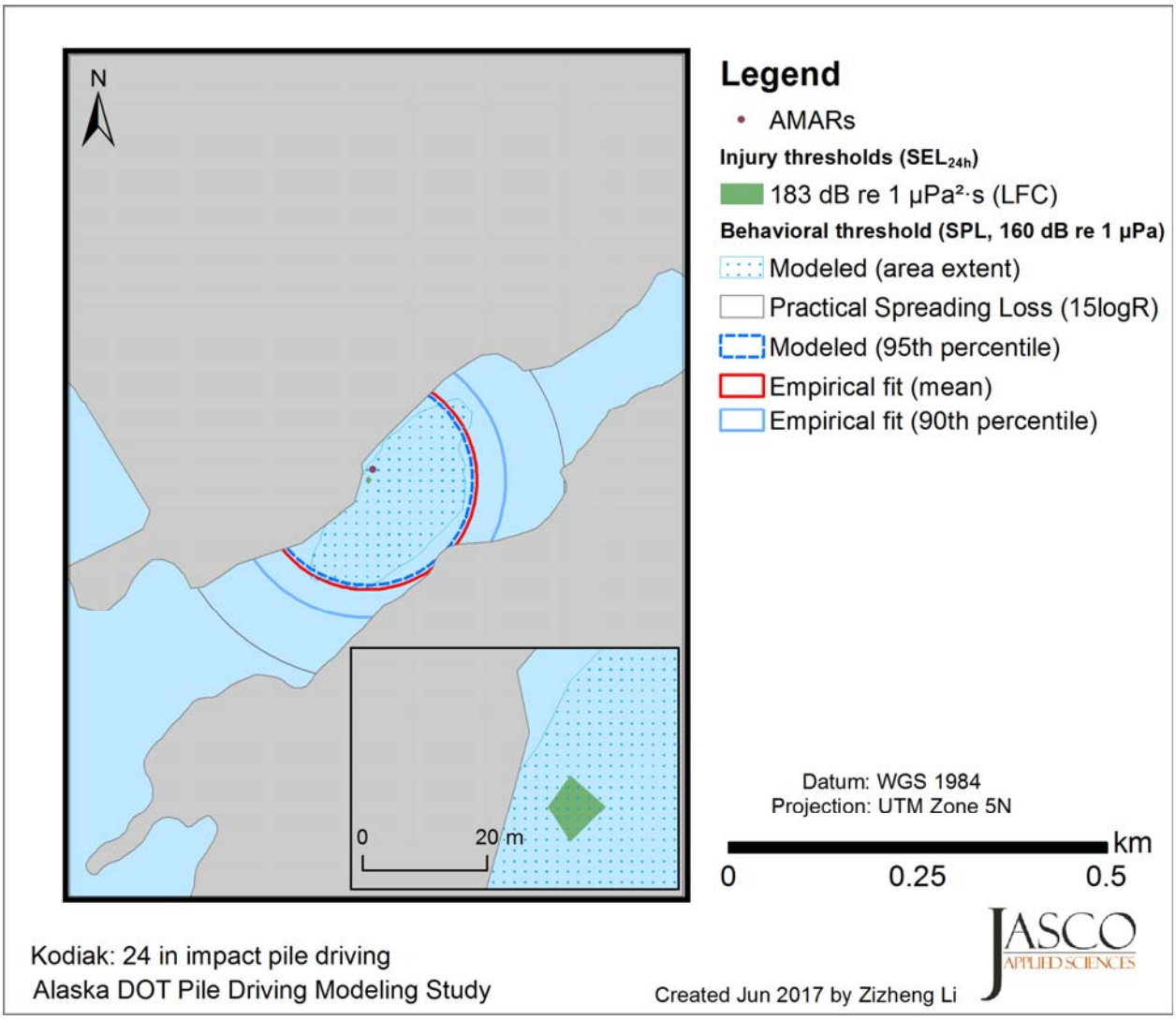

Figure 25. Kodiak: Contours to thresholds for marine mammal injury (where exceeded) and behavioral disturbance from impulsive sources for impact pile driving. The inset shows a close-up of sound fields around the pile location. Also shown are circles of radii corresponding to the mean and 90th percentile behavioral impact threshold distances derived from the empirical research project and from the $R_{95\%}$ modeled distance as well as from a Practical Spreading Loss model assumption and the mean measured source level. Solid circles marked AMARs are the measurement locations from the empirical research project..

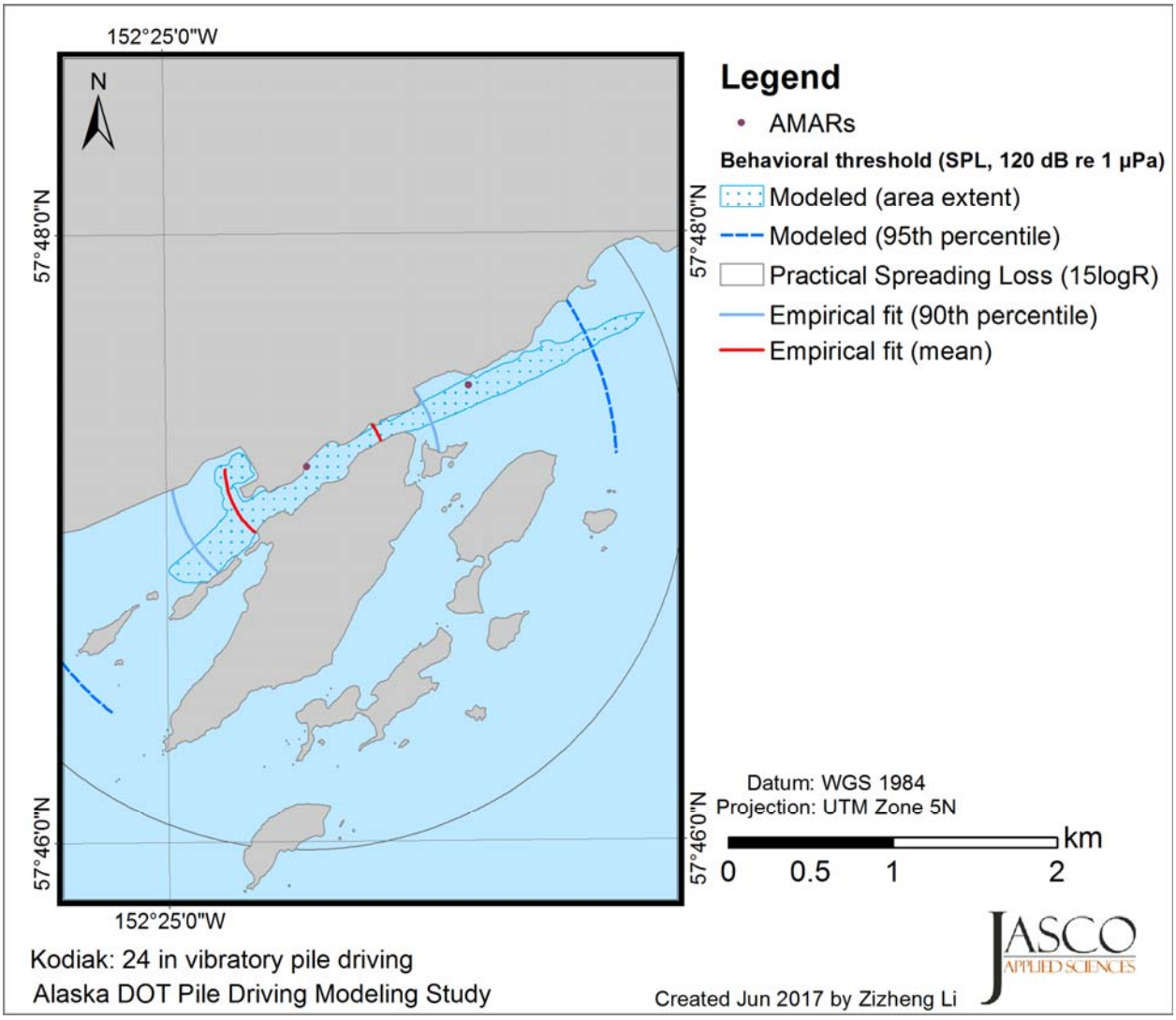

Figure 26. Kodiak: Contours to thresholds for behavioral disturbance from non-impulsive sources for vibratory pile driving Circles of radii correspond to the mean and 90th percentile behavioral impact threshold distances derived from the empirical research project and from the $R_{95\%}$ modeled distance.

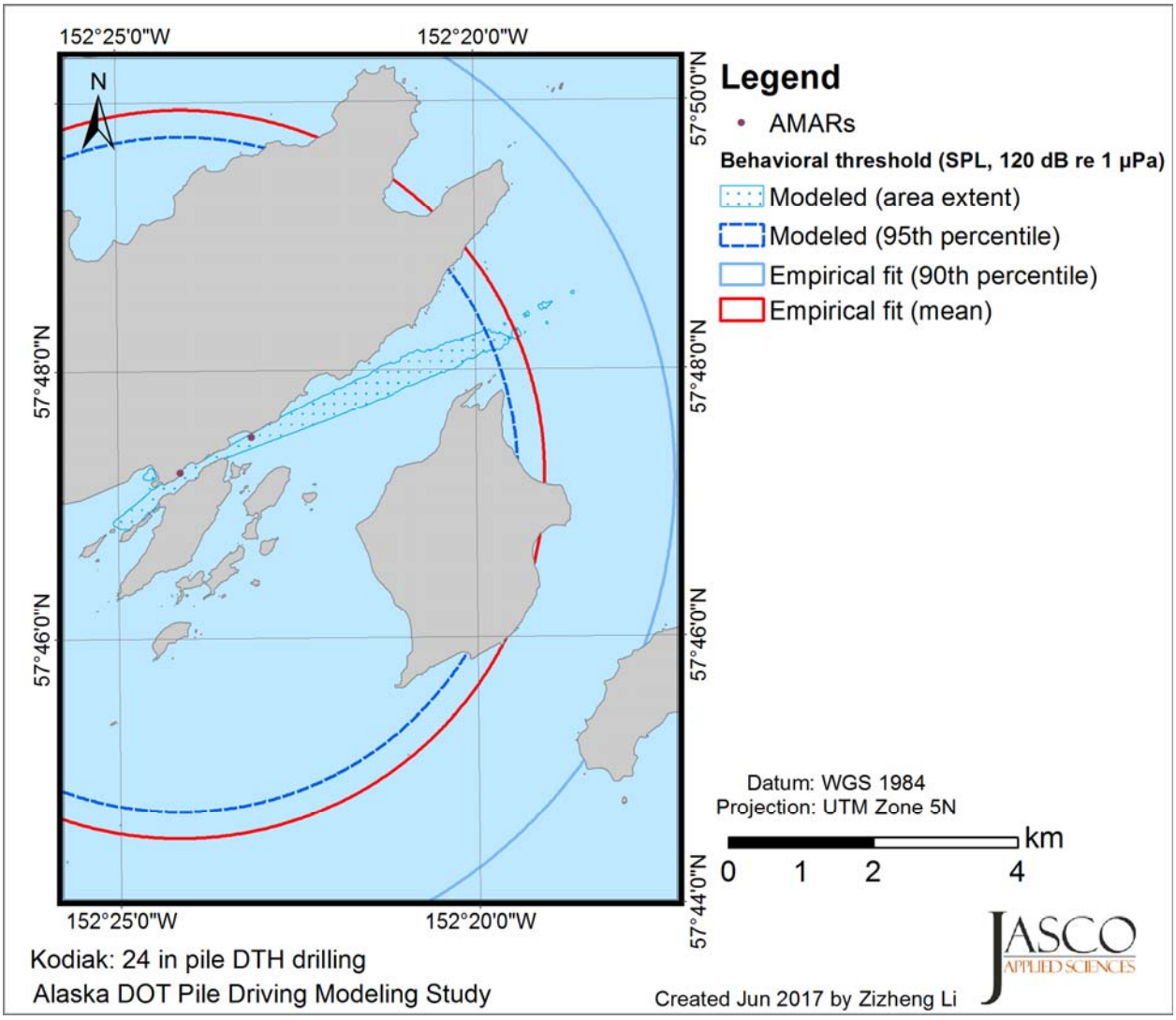

Figure 27. Kodiak: Contours to thresholds for behavioral disturbance from non-impulsive sources for drilling. Circles of radii correspond to the mean and 90th percentile behavioral impact threshold distances derived from the empirical research project and from the $R_{95\%}$ modeled distance.

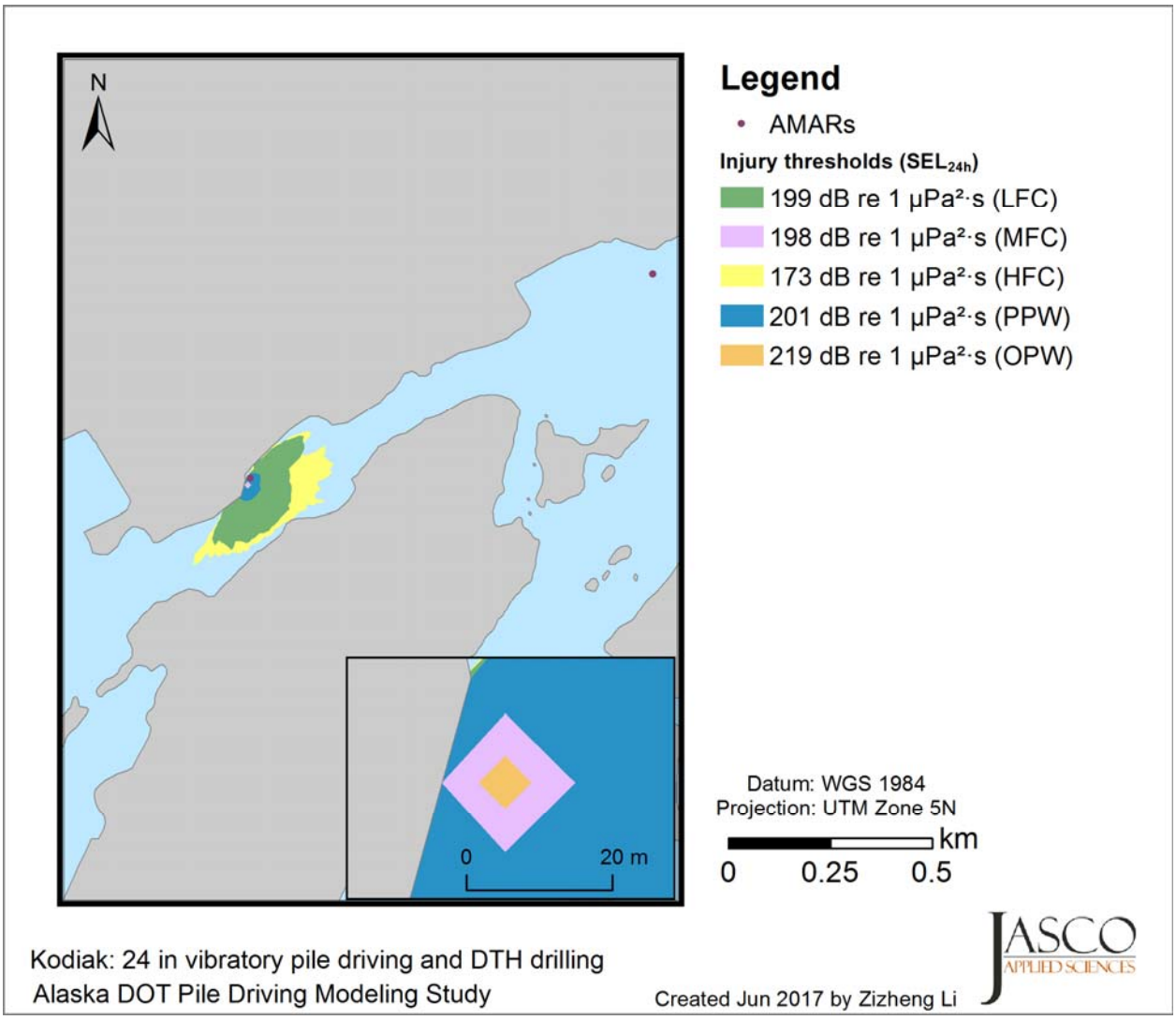

Figure 28. Kodiak: Contours to thresholds for marine mammal injury from non-impulsive sources for vibratory pile driving and drilling. The inset is a close-up of sound fields around the pile location.

7. Distances to Criteria Thresholds

The maximum (R_{max}) and 95th percentile ($R_{95\%}$) distances to the regulated marine mammal impact thresholds were calculated from the modeled sound level contours from Section 6and are tabulated in this section. Mean and 90th percentile distances to same thresholds, computed from the empirical measurement research project, are also tabulated for comparison. Distances to SPL thresholds of 190 and 180 dB re 1 µPa are included in the tables because when the empirical research project was underway those were the thresholds against which NMFS assessed potential for Level A harassment for pinnipeds and cetaceans.

7.1. Auke Bay

Table 6. Auke Bay: Distance in meters to SPL thresholds based on NMFS (2013) criteria determined from modeling and from best-fit transmission loss coefficient and SPLs at the closest measurement range (90th percentile and mean) from the empirical research project.

Threshold (SPL, dB re 1 µPa)	**Modeled**		**From Measurements**	
	R_{max}	$R_{95\%}$	90th Percentile Distance	Mean Distance
Impact driving 30” piles				
190	14	14	14±2	12±2
180	104	91	67±5	57±5
160	3698	2956	1567*±44	1338*±31
Vibratory driving 30” piles				
120	8482	7341	16126*±1507	10257*±455

*Extrapolated beyond maximum measurement range.

Table 7. Auke Bay: Range in meters to onset of injury, based on NMFS (2016) criteria. LFC = low-frequency cetaceans, MFC = mid-frequency cetaceans, HFC = high-frequency cetaceans, PPW = Phocid pinnipeds in water, OPW = Otariid pinnipeds in water.

Weighting	**Modeled**					**From Measurements**		
	Impact			Vibratory		Impact		Vibratory
	SEL_{24h}		Peak	SEL_{24h}		SEL_{24h}	Peak	SEL_{24h}
	R_{max}	$R_{95\%}$	R_{max}	R_{max}	R_{95}			
LFC	2966	1315	4	14	14	740	4	15
MFC	0	0	0	0	0	13	1	6
HFC	860	830	113	0	0	557	31	82
PPW	155	132	5	0	0	122	5	9
OPW	0	0	0	0	0	8	1	1

7.2. Kake

Table 8. Kake: Distance in meters to SPL thresholds, determined from modeling and from best-fit transmission loss coefficient and SPLs at the closest measurement range (90th percentile and mean). Threshold distances from measurements are maximized over the levels from the east and west restraint piles.

Threshold (SPL, dB re 1 µPa)	Modeled		From Measurements	
	R_{max}	$R_{95\%}$	90th Percentile Distance	Mean Distance
Impact driving 30” piles				
190	14	14	27	20
180	78	73	86	66
160	1076	868	897	685
Vibratory driving 30” piles				
120	1470	1281	1207*	825

*Extrapolated beyond maximum measurement range.

Table 9. Kake: Range in meters to onset of hearing injury, based on NMFS (2016) criteria. LFC = low-frequency cetaceans, MFC = mid-frequency cetaceans, HFC = high-frequency cetaceans, PPW = Phocid pinnipeds in water, OPW = Otariid pinnipeds in water.

Weighting	Modeled					From Measurements		
	Impact			Vibratory		Impact		Vibratory
	SEL_{24h}		Peak	SEL_{24h}		SEL_{24h}	Peak	SEL_{24h}
	R_{max}	$R_{95\%}$	R_{max}	R_{max}	R_{95}			
LFC	262	248	2	0	0	124	4	2
MFC	0	0	0	0	0	7	1	0
HFC	228	192	51	0	0	164	31	2
PPW	51	45	3	0	0	37	5	0
OPW	0	0	0	0	0	4	1	0

7.3. Ketchikan

Table 10. Ketchikan: Distance to SPL thresholds, determined from modeling and from best-fit transmission loss coefficient and SPLs at the closest measurement range (90th percentile and mean). Threshold distances and source levels obtained from measurements are maximized over data from all piles monitored for each activity.

Threshold (SPL, dB re 1 µPa)	Modeled		From Measurements	
	R_{max}	$R_{95\%}$	90th Percentile Distance	Mean Distance
Impact driving 30” piles				
190	40	32	27.4	22.8

Threshold (SPL, dB re 1 µPa)	Modeled		From Measurements	
	R_{max}	$R_{95\%}$	90th Percentile Distance	Mean Distance
180	245	187	127	105
160	4566	3062	2703*	2250*
Vibratory driving 30” piles				
120	9334	7241	120147*	61383*

*Extrapolated far beyond maximum measurement range.

Table 11. Ketchikan: Range in meters to onset of hearing injury, based on NMFS (2016). LFC = low-frequency cetaceans, MFC = mid-frequency cetaceans, HFC = high-frequency cetaceans, PPW = Phocid pinnipeds in water, OPW = Otariid pinnipeds in water.

Weighting	Modeled					From Measurements		
	Impact			Vibratory		Impact		Vibratory
	SEL_{24h}		Peak	SEL_{24h}		SEL_{24h}	Peak	SEL_{24h}
	R_{max}	$R_{95\%}$	R_{max}	R_{max}	R_{95}			
LFC	4547	2962	18	63	54	1288*	< 10	10
MFC	41	32	3	0	0	21	< 10	< 10
HFC	1571	1092	110	10	10	746	46	11
PPW	630	504	21	0	0	212	< 10	< 10
OPW	32	32	1	0	0	13	< 10	< 10

*Extrapolated beyond maximum measurement range.

7.4. Kodiak

Table 12. Kodiak: Distance to SPL thresholds, determined from modeling and from best-fit transmission loss coefficient and SPLs at the closest measurement range (90th percentile and mean). Threshold distances and source levels obtained from measurements are maximized over data from all piles monitored for each activity.

Threshold (SPL, dB re 1 µPa)	Modeled		From Measurements	
	R_{max}	$R_{95\%}$	90th Percentile Distance	Mean Distance
Impact driving 30” piles				
190	0	0	6.1	4.8
180	0	0	19	15
160	158	139	183	145
Vibratory driving 30” piles				
120	2273	1898	821	490
Drilling 24” piles				
120	6013	4678	6846*	5049*

*Extrapolated beyond maximum measurement range.

Table 13. Kodiak: Range in meters to onset of injury. For the estimation of ranges based on measurements, drilling and vibratory hammer setting were considered together for exposure estimates within the continuous category. LFC = low-frequency cetaceans, MFC = mid-frequency cetaceans, HFC = high-frequency cetaceans, PPW = Phocid pinnipeds in water, OPW = Otariid pinnipeds in water.

Weighting	Modeled					From Measurements				
	Impact			Continuous		Impact		Continuous		
	SEL_{24h}		Peak	SEL_{24h}		SEL_{24h}	Peak	Day1	Day 2	Day 3
	R_{max}	$R_{95\%}$	R_{max}	R_{max}	$R_{95\%}$					
LFC	0	0	0	177	148	5	1	3	35	24
MFC	0	0	0	0	0	1	0	1	4	2
HFC	0	0	2	234	192	15	6	10	40	30
PPW	0	0	0	36	36	2	1	2	12	9
OPW	0	0	0	0	0	0	0	0	2	1

8. Discussion and Summary

The modeled sound levels at Auke Bay, Kake and Ketchikan were generally within the statistical distribution of the measured levels, occasionally exceeding the measured values. The measured sound levels for impact and vibratory pile driving at Kodiak were consistently overestimated by the model, by between 4 and 15 dB. This is suspected to be a result of the model's treatment of the shallow bedrock layer at this location (Appendix C).

Except at Kodiak, the broadband modeled SEL for impact pile driving was within 1 dB of the maximum measured SEL at the closest measurement range for each location, it was within 3 dB of the mean measured level (Table 14). For vibratory pile driving, the modeled SEL was within 3 dB of the mean measured level at Auke Bay and Kake but the difference from the maximum measured value was as much as 13 dB. The modeled SEL for vibratory pile driving at Ketchikan was within 4 dB of the maximum measured level at the closest measurement range, but was 13 dB higher than the mean measured level at that distance. The plots of sound pressure levels versus range from Section 5 showed similar trends for the differences between measured and modeled peak and SPL values at each location as has just been described for the SEL values.

Table 14 Broadband SEL (dB re 1 μPa^2s) for impact (single strike) and vibratory pile driving, measured and modeled, at the closest measurement location.

	Impact			Vibratory		
	Measured Max	**Measured Mean**	**Modeled**	**Measured Max**	**Measured Mean**	**Modeled**
Auke Bay (7.0 m range)	182	180	181	184	172	171
Kake (9.5 m range)	184	181	183	171	160	163
Ketchikan (17.3 m range)	180	178	181	164	155	168
Kodiak (16.0 m range)	164	163	171	157	145	161

Our modeling procedure did include some iterative refinement whereby model inputs were adjusted to better align the output with data from all measurement ranges. We tuned the source model to match the upper reaches of the measured levels at close range, following the paradigm of the precautionary principle where we strive for the model to yield a conservative approximation of possible outcomes, given uncertainty of the input parameters.

Source levels were primarily adjusted by varying the simulated pile penetration rate as a surrogate of the hammer efficiency, which can be affected by things like reduced fuel and power settings or the presence of a pile cap. The GRLWEAP model allows tuning of the fuel setting for some model hammers; when possible, this was adjusted as necessary to optimize the agreement with the near source data. This model refinement step is not possible for projects at sites where there are no empirical data available for comparison. It is also often impossible to know in advance what some of the detailed hammer settings will be, so predictive acoustic modeling should aim to select input parameters that will yield conservative estimates of the sound field, without grossly overestimating the expected conditions.

The model calculations yielded distances to the marine mammal impact thresholds that were typically larger than those from the empirical estimates, particularly for the Level A harassment thresholds. This follows from the fact that the modeled levels tended to exceed the mean measured levels, and because the model considered the maximum sound level over all depths but the measurements apply only to the sound levels at the seafloor. Modeled distances to the PK thresholds for Level A harassment also tended to exceed the distances from the empirical data because the empirical estimates were approximated assuming spherical spreading loss for the PK levels. The modeling indicates that this was not a good approximation of the propagation conditions for most of these locations, largely due to the down-sloping bathymetry near the piles that supported relatively-unattenuated propagation of the mach cone. The model-data agreement for PK levels was best at Kake, where the slope of the seafloor is shallower than the mach cone angle, and the transmission loss at short ranges more closely resembled the spherical spreading loss assumption for PK.

The summation of the single-strike levels (or per-second levels, for vibratory pile driving and drilling) over many hammer strikes (or many seconds) compounds the degree to which the model precautionarily estimates the Level A impact threshold distances. Furthermore, the cumulative SEL calculation from empirical data accounts for the inter-strike (or temporal, for vibratory pile driving) variation of the source sound levels, whereas the modeling approach assumes a constant, and maximal, level for each hammer strike (or each second of vibratory pile driving and drilling). Thus, the modeling approach yields a more precautionary estimate of the SEL_{24h}.

The modeled source spectral distributions for impact pile driving were quite similar to measured data collected near (~10 m) the piles. The higher frequency components from vibratory pile driving were not simulated as accurately, but the model gave similar results to the data at the dominant, fundamental frequencies. The model-data agreement at higher frequencies was improved by introducing non-linearity to the PDSM source signature. Nevertheless, the model-data agreement of the broadband levels was very good near 1 km.

Distances to the Level B thresholds tended to extend further than the maximum measurement range from the empirical research project. Hence the empirical estimates, extrapolated from the measured data, were highly uncertain and were, in some cases, unrealistically large. The extrapolated threshold distances were calculated using the transmission loss determined between the two measurement points to extrapolate to longer ranges. Since transmission loss is range dependent, the trend between the two measurements points is not likely to be appropriate for long-range propagation beyond the furthest point. This modeling project has provided the range-dependent transmission loss information that allows us to calculate these distances more accurately, yielding shorter distances to these thresholds.

The most extreme illustration of the unrealistically large distances from the empirical fit was at Ketchikan, where the distances to the 120 dB SPL threshold for vibratory piling estimated from the empirical research project were approximately 120 km from the 90th percentile and 61 km from the mean measured levels. These distances were extrapolated, using the empirical transmission loss fit, well beyond the maximum measurement range of approximately 950 m (Denes et al. 2016). The modeled distance to the 120 dB SPL threshold for vibratory pile driving at Ketchikan was more realistic - 9.3 km based on the R_{max} or 7.2 km from the $R_{95\%}$. Similarly, the mean empirical data from Auke Bay yielded a 10 km distance to the 120 dB re 1 µPa SPL threshold, or 16 km from the 90th percentile measured data. The modeled distances to the 120 dB re 1 µPa SPL threshold were 8.4 km for R_{max} and 7.3 km for $R_{95\%}$.

This modeling effort has demonstrated that the model can simulate underwater pile driving sound levels accurately to within the range of variability of measured data. The source model accurately simulates the source signature for impact pile driving and adequately replicates the signature for vibratory pile driving to accurately predict broadband sound levels at a distance from the pile. When input parameters are selected appropriately, precautionary, yet realistic, estimates of the distances for marine mammal impact threshold exceedances can be obtained. This modeling approach is a useful tool for estimating zones of ensonification for future projects at sites that lack measured data.

Glossary

1/3-octave-band
Non-overlapping passbands that are one-third of an octave wide (where an octave is a doubling of frequency). Three adjacent 1/3-octave-bands comprise one octave. One-third-octave-bands become wider with increasing frequency. Also see octave.

azimuth
A horizontal angle relative to a reference direction, which is often magnetic north or the direction of travel. In navigation, it is also called bearing.

bandwidth
The range of frequencies over which a sound occurs. Broadband refers to a source that produces sound over a broad range of frequencies (e.g., seismic airguns, vessels) whereas narrowband sources produce sounds over a narrow frequency range (e.g., sonar) (ANSI/ASA S1.13-2005 R2010).

broadband sound level
The total sound pressure level measured over a specified frequency range. If the frequency range is unspecified, it refers to the entire measured frequency range.

cetacean
Any animal in the order Cetacea. These are aquatic, mostly marine mammals and include whales, dolphins, and porpoises.

compressional wave
A mechanical vibration wave in which the direction of particle motion is parallel to the direction of propagation. Also called primary wave or P-wave.

continuous sound
A sound whose sound pressure level remains above ambient sound during the observation period (ANSI/ASA S1.13-2005 R2010). A sound that gradually varies in intensity with time, for example, sound from a marine vessel.

decibel (dB)
One-tenth of a bel. Unit of level when the base of the logarithm is the tenth root of ten, and the quantities concerned are proportional to power (ANSI S1.1-1994 R2004).

ensonified
Exposed to sound.

fast Fourier transform (FFT)
A computationally efficiently algorithm for computing the discrete Fourier transform.

frequency
The rate of oscillation of a periodic function measured in cycles-per-unit-time. The reciprocal of the period. Unit: hertz (Hz). Symbol: *f*. 1 Hz is equal to 1 cycle per second.

hearing group
Groups of marine mammal species with similar hearing ranges. Commonly defined functional hearing groups include low-, mid-, and high-frequency cetaceans, pinnipeds in water, and pinnipeds in air.

geoacoustic
Relating to the acoustic properties of the seabed.

harmonic
A sinusoidal sound component that has a frequency that is an integer multiple of the frequency of a sound to which it is related. For example, the second harmonic of a sound has a frequency that is double the fundamental frequency of the sound.

hearing threshold
The sound pressure level that is barely audible for a given individual in the absence of significant background noise during a specific percentage of experimental trials.

hertz (Hz)
A unit of frequency defined as one cycle per second.

high-frequency cetacean (HFC)
The functional hearing group that represents odontocetes specialized for using high frequencies.

hydrophone
An underwater sound pressure transducer. A passive electronic device for recording or listening to underwater sound.

impulsive sound
Sound that is typically brief and intermittent with rapid (within a few seconds) rise time and decay back to ambient levels (NOAA 2013, ANSI S12.7-1986 R2006). For example, seismic airguns and impact pile driving.

low-frequency cetacean (LFC)
The functional hearing group that represents mysticetes (baleen whales).

masking
Obscuring of sounds of interest by sounds at similar frequencies.

median
The 50th percentile of a statistical distribution.

mid-frequency cetacean (MFC)
The functional hearing group that represents some odontocetes (dolphins, toothed whales, beaked whales, and bottlenose whales).

mysticete
Mysticeti, a suborder of cetaceans, use their baleen plates, rather than teeth, to filter food from water. They are not known to echolocate, but use sound for communication. Members of this group include rorquals (Balaenopteridae), right whales (Balaenidae), and gray whales (*Eschrichtius robustus*).

non-impulsive sound
Sound that is broadband, narrowband or tonal, brief or prolonged, continuous or intermittent, and typically does not have a high peak pressure with rapid rise time (typically only small fluctuations in decibel level) that impulsive signals have (ANSI/ASA S3.20-1995 R2008). For example, marine vessels, aircraft, machinery, construction, and vibratory pile driving (NIOSH 1998, NOAA 2015).

octave
The interval between a sound and another sound with double or half the frequency. For example, one octave above 200 Hz is 400 Hz, and one octave below 200 Hz is 100 Hz.

odontocete
The presence of teeth, rather than baleen, characterizes these whales. Members of the Odontoceti are a suborder of cetaceans, a group comprised of whales, dolphins, and porpoises. The toothed whales' skulls are mostly asymmetric, an adaptation for their echolocation. This group includes sperm whales, killer whales, belugas, narwhals, dolphins, and porpoises.

otariid
A common term used to describe members of the Otariidae, eared seals, commonly called sea lions and fur seals. Otariids are adapted to a semi-aquatic life; they use their large fore flippers for propulsion. Their ears distinguish them from phocids. Otariids are one of the three main groups in the superfamily Pinnipedia; the other two groups are phocids and walrus.

parabolic equation method
A computationally-efficient solution to the acoustic wave equation that is used to model transmission loss. The parabolic equation approximation omits effects of back-scattered sound, simplifying the computation of transmission loss. The effect of back-scattered sound is negligible for most ocean-acoustic propagation problems.

peak pressure level (PK)
The maximum instantaneous sound pressure level, in a stated frequency band, within a stated period. Also called zero-to-peak pressure level. Unit: decibel (dB).

percentile level, exceedance
The sound level exceeded *n* % of the time during a measurement.

permanent threshold shift (PTS)
A permanent loss of hearing sensitivity caused by excessive noise exposure. PTS is considered auditory injury.

phocid
A common term used to describe all members of the family Phocidae. These true/earless seals are more adapted to in-water life than are otariids, which have more terrestrial adaptations. Phocids use their hind flippers to propel themselves. Phocids are one of the three main groups in the superfamily Pinnipedia; the other two groups are otariids and walrus.

pinniped
A common term used to describe all three groups that form the superfamily Pinnipedia: phocids (true seals or earless seals), otariids (eared seals or fur seals and sea lions), and walrus.

point source
A source that radiates sound as if from a single point (ANSI S1.1-1994 R2004).

pressure, acoustic
The deviation from the ambient hydrostatic pressure caused by a sound wave. Also called overpressure. Unit: pascal (Pa). Symbol: *p*.

pressure, hydrostatic
The pressure at any given depth in a static liquid that is the result of the weight of the liquid acting on a unit area at that depth, plus any pressure acting on the surface of the liquid. Unit: pascal (Pa).

received level
The sound level measured at a receiver.

rms
root-mean-square.

shear wave
A mechanical vibration wave in which the direction of particle motion is perpendicular to the direction of propagation. Also called secondary wave or S-wave. Shear waves propagate only in solid media, such as sediments or rock. Shear waves in the seabed can be converted to compressional waves in water at the water-seabed interface.

signature
Pressure signal generated by a source.

sound
A time-varying pressure disturbance generated by mechanical vibration waves travelling through a fluid medium such as air or water.

sound exposure
Time integral of squared, instantaneous frequency-weighted sound pressure over a stated time interval or event. Unit: pascal-squared second ($Pa^2 \cdot s$) (ANSI S1.1-1994 R2004).

sound exposure level (SEL)
A cumulative measure related to the sound energy in one or more pulses. Unit: dB re 1 $\mu Pa^2 \cdot s$. SEL is expressed over the summation period (e.g., per-pulse SEL [for airguns], single-strike SEL [for pile drivers], 24-hour SEL).

sound field
Region containing sound waves (ANSI S1.1-1994 R2004).

sound intensity
Sound energy flowing through a unit area perpendicular to the direction of propagation per unit time.

sound pressure level (SPL)
The decibel ratio of the time-mean-square sound pressure, in a stated frequency band, to the square of the reference sound pressure (ANSI S1.1-1994 R2004).

For sound in water, the reference sound pressure is one micropascal (p_0 = 1 µPa) and the unit for SPL is dB re 1 µPa:

$$\mathrm{SPL} = 10\log_{10}\left(p^2 / p_0^2\right) = 20\log_{10}\left(p / p_0\right)$$

Unless otherwise stated, SPL refers to the root-mean-square sound pressure level. See also 90% sound pressure level and fast-average sound pressure level. Non-rectangular time window functions can be applied during calculation of the rms value, in which case the SPL unit should identify the window type.

sound speed profile
The speed of sound in the water column as a function of depth below the water surface.

source level (SL)
The sound level measured in the far-field and scaled back to a standard reference distance of 1 metre from the acoustic centre of the source. Unit: dB re 1 µPa @ 1 m (sound pressure level) or dB re 1 $\mu Pa^2 \cdot s$ (sound exposure level).

spectrum
An acoustic signal represented in terms of its power (or energy) distribution compared with frequency.

temporary threshold shift (TTS)
Temporary loss of hearing sensitivity caused by excessive noise exposure.

transmission loss (TL)
The decibel reduction in sound level between two stated points that results from sound spreading away from an acoustic source subject to the influence of the surrounding environment. Also called propagation loss.

Literature Cited

[NIOSH] National Institute for Occupational Safety and Health. 1998. *Criteria for a recommended standard: Occupational noise exposure*. Document Number 98-126. U.S. Department of Health and Human Services, NIOSH, Cincinnati, Ohio. 122 pp.

[NMFS] National Marine Fisheries Service. 2013. *Marine Mammals: Interim Sound Threshold Guidance* (webpage). National Marine Fisheries Service, National Oceanic and Atmospheric Administration, U.S. Department of Commerce. http://www.westcoast.fisheries.noaa.gov/protected_species/marine_mammals/threshold_guidance.html.

[NMFS] National Marine Fisheries Service. 2016. *Technical Guidance for Assessing the Effects of Anthropogenic Sound on Marine Mammal Hearing: Underwater Acoustic Thresholds for Onset of Permanent and Temporary Threshold Shifts*. U.S. Department of Commerce, NOAA. NOAA Technical Memorandum NMFS-OPR-55. 178 pp. http://www.nmfs.noaa.gov/pr/acoustics/Acoustic%20Guidance%20Files/opr-55_acoustic_guidance_tech_memo.pdf.

[NOAA] National Oceanic and Atmospheric Administration. 2013. *Draft guidance for assessing the effects of anthropogenic sound on marine mammals: Acoustic threshold levels for onset of permanent and temporary threshold shifts*, December 2013, 76 pp. Silver Spring, Maryland: NMFS Office of Protected Resources. http://www.nmfs.noaa.gov/pr/acoustics/draft_acoustic_guidance_2013.pdf.

[NOAA] National Oceanic and Atmospheric Administration. 2015. *Draft guidance for assessing the effects of anthropogenic sound on marine mammal hearing: Underwater acoustic threshold levels for onset of permanent and temporary threshold shifts*, July 2015, 180 pp. Silver Spring, Maryland: NMFS Office of Protected Resources. http://www.nmfs.noaa.gov/pr/acoustics/draft%20acoustic%20guidance%20July%202015.pdf.

[NOAA] National Oceanic and Atmospheric Administration. 2016. *NOAA Electronic Navigational Chart* (webpage). National Ocean Service. http://www.charts.noaa.gov/InteractiveCatalog/nrnc.shtml#mapTabs-2.

[NOAA] National Oceanic and Atmospheric Administration (US), [NOS] National Ocean Service, and [CO-OPS] Center for Operational Oceanographic Products and Services. 2017. NOAA Tide Predictions. Center for Operational Oceanographic Products and Services, National Oceanic and Atmospheric Administration, US Department of Commerce. https://tidesandcurrents.noaa.gov/noaatidepredictions.html?id=9457261&legacy=1 (Accessed Jun 4, 2017).

Aerts, L., M. Blees, S. Blackwell, C. Greene, K. Kim, D. Hannay, and M. Austin. 2008. *Marine mammal monitoring and mitigation during BP Liberty OBC seismic survey in Foggy Island Bay, Beaufort Sea, July-August 2008: 90-day report*. Document Number LGL Report P1011-1. Report by LGL Alaska Research Associates Inc., LGL Ltd., Greeneridge Sciences Inc. and JASCO Applied Sciences for BP Exploration Alaska. 199 pp. http://www.nmfs.noaa.gov/pr/pdfs/permits/bp_liberty_monitoring.pdf.

Alaska Department of Transportation and Public Facilities, Engineering and Operations, Headquarters Materials Section, Anchorage Alaska. 1996. *Engineering Geology and Soils Report Auke Bay Ferry Terminal Staging Area Materials Investigation*. Project No. NH-0933(006), State Project No. 75227, Southeast Region, Anchorage, AK. 38 pp.

ANSI S12.7-1986. R2006. *American National Standard Methods for Measurements of Impulsive Noise*. American National Standards Institute, New York.

ANSI S1.1-1994. R2004. *American National Standard Acoustical Terminology*. American National Standards Institute, New York.

ANSI/ASA S1.13-2005. R2010. *American National Standard Measurement of Sound Pressure Levels in Air*. American National Standards Institute and Acoustical Society of America, New York.

ANSI/ASA S3.20-1995. R2008. *American National Standard Bioacoustical Terminology*. American National Standards Institute and Acoustical Society of America, New York.

Briggs, K.B. and K.M. Fischer. 1992. *Geoacoustic Model of the Strait of Korea*. Document Number AD-A247 205. 51 pp.

Brocher, T.M. 2005. *Compressional and shear wave velocity versus depth in the San Francisco Bay Area, California: Rules for USGS Bay Area Velocity Model 05.0. 0*. Report Number Open-File Report 05–1317.

Buckingham, M.J. 2005. Compressional and shear wave properties of marine sediments: Comparisons between theory and data. *Journal of the Acoustical Society of America* 117(1): 137-152.

Collins, M.D. 1993. A split-step Padé solution for the parabolic equation method. *Journal of the Acoustical Society of America* 93(4): 1736-1742.

Collins, M.D., R.J. Cederberg, D.B. King, and S. Chin-Bing. 1996. Comparison of algorithms for solving parabolic wave equations. *Journal of the Acoustical Society of America* 100(1): 178-182.

Dames & Moore. 1973. *Soils and Foundation Investigation Proposed Ferry Terminal, Kake, Alaska*. Report for State of Alaska, Department of Public Works, Job 8514-019-20.

Denes, S., G. Warner, M. Austin, and A. MacGillivray. 2016. *Hydroacoustic Pile Driving Noise Study – Comprehensive Report*. Document Number 001285, Version 2.0. Technical report by JASCO Applied Sciences for Alaska Department of Transportation & Public Facilities.

Duncan, A., A. Gavrilov, and F. Li. 2009. *Acoustic propagation over limestone seabeds*. *Proceedings of Acoustics 2009: Research to Counsulting, Annual Conference of the Australian Acoustical Society*. University of Adelaide, pp. 1-6.

Finneran, J.J. 2015. *Auditory weighting functions and TTS/PTS exposure functions for cetaceans and marine carnivores*. San Diego: SSC Pacific.

Finneran, J.J. 2016. *Auditory weighting functions and TTS/PTS exposure functions for marine mammals exposed to underwater noise*. Technical Report. 49 pp.

Funk, D., D. Hannay, D. Ireland, R. Rodrigues, and W. Koski (eds.). 2008. *Marine mammal monitoring and mitigation during open water seismic exploration by Shell Offshore Inc. in the Chukchi and Beaufort Seas, July–November 2007: 90-day report*. LGL Report P969-1. Prepared by LGL Alaska Research Associates Inc., LGL Ltd., and JASCO Research Ltd. for Shell Offshore Inc., National Marine Fisheries Service (US), and US Fish and Wildlife Service. 218 pp.

Hamilton, E.L. 1980. Geoacoustic modeling of the sea floor. *Journal of the Acoustical Society of America* 68(5): 1313-1340.

Hannay, D. and R. Racca. 2005. *Acoustic Model Validation*. Document Number 0000-S-90-04-T-7006-00-E, Revision 02. Technical report for Sakhalin Energy Investment Company Ltd. by JASCO Research Ltd. 34 pp.

Ireland, D.S., R. Rodrigues, D. Funk, W. Koski, and D. Hannay. 2009. *Marine mammal monitoring and mitigation during open water seismic exploration by Shell Offshore Inc. in the Chukchi and Beaufort Seas, July–October 2008: 90-Day Report*. Document Number LGL Report P1049-1. 277 pp.

Jensen, F.B., W.A. Kuperman, M.B. Porter, and H. Schmidt. 2011. *Computational Ocean Acoustics*. 2nd edition. AIP Series in Modern Acourics and Signal Processing. AIP Press - Springer, New York. 794 pp.

King, E.C., A.M. Smith, T. Murray, and G. Stuart. 2008. Glacier-bed characteristics of midtre Lovénbreen, Svalbard, from high-resolution seismic and radar surveying. *Journal of Glaciology* 54(184): 145-156.

MacGillivray, A. 2014. A model for underwater sound levels generated by marine impact pile driving. *Proceedings of Meetings on Acoustics* 20(1): 045008. http://scitation.aip.org/content/asa/journal/poma/20/1/10.1121/2.0000030.

MacGillivray, A.O. and N.R. Chapman. 2012. Modeling underwater sound propagation from an airgun array using the parabolic equation method. *Canadian Acoustics* 40(1): 19-25. http://jcaa.caa-aca.ca/index.php/jcaa/article/view/2502.

Martin, B., K. Broker, M.-N.R. Matthews, J. MacDonnell, and L. Bailey. 2015. *Comparison of measured and modeled air-gun array sound levels in Baffin Bay, West Greenland. OceanNoise 2015*, 11-15 May, Barcelona, Spain.

Nedwell, J.R. and A.W. Turnpenny. 1998. The use of a generic frequency weighting scale in estimating environmental effect. *Workshop on Seismics and Marine Mammals*. 23–25th June 1998, London, U.K.

Nedwell, J.R., A.W.H. Turnpenny, J. Lovell, S.J. Parvin, R. Workman, and J.A.L. Spinks. 2007. *A validation of the dB_{ht} as a measure of the behavioural and auditory effects of underwater noise*. Report No. 534R1231 prepared by Subacoustech Ltd. for the UK Department of Business, Enterprise and Regulatory Reform under Project No. RDCZ/011/0004. www.subacoustech.com/information/downloads/reports/534R1231.pdf.

NOAA/NMFS Juneau Consolidated Facility. 1998. *Fisheries Management Operation, 'Vision for 2005': Environmental Impact Statement*. 4 pp. https://books.google.ca/books/about/NOAA_NMFS_Juneau_Consolidated_Facility_F.html?id=IiM3AQAAMAAJ&redir_esc=y.

O'Neill, C., D. Leary, and A. McCrodan. 2010. Sound Source Verification. (Chapter 3) *In* Blees, M.K., K.G. Hartin, D.S. Ireland, and D. Hannay (eds.). *Marine mammal monitoring and mitigation during open water seismic exploration by Statoil USA E&P Inc. in the Chukchi Sea, August-October 2010: 90-day report*. LGL Report P1119. Prepared by LGL Alaska Research Associates Inc., LGL Ltd., and JASCO Applied Sciences Ltd. for Statoil USA E&P Inc., National Marine Fisheries Service (US), and US Fish and Wildlife Service. pp 1-34.

Pile Dynamics, Inc. 2010. GRLWEAP.

Quijano, J., M. Woods, C. O'Neill, and S. Hipsey. 2016. *Prince Rupert Gas Transmission Acoustics Study: Underwater Noise Modelling of Pile Driving Activities*. Document Number 01122, Version 2.0. Technical report by JASCO Applied Sciences for Stantec Consulting Ltd. 66 pp.

R&M Consultants, I. 2013. *Foundation Geology Report: Kodiak Ferry Terminal &Dock Improvements (AKSAS #68938) Kodiak, Alaska* Report Number 1848.01. Foundation Geology Report prepared for the Alaska Department of Transportation & Public Facilities. 44 pp.

Racca, R., A. Rutenko, K. Bröker, and M. Austin. 2012a. A line in the water - design and enactment of a closed loop, model based sound level boundary estimation strategy for mitigation of behavioural impacts from a seismic survey. *11th European Conference on Underwater Acoustics 2012*. Volume 34(3), Edinburgh, United Kingdom.

Racca, R., A. Rutenko, K. Bröker, and G. Gailey. 2012b. *Model based sound level estimation and in-field adjustment for real-time mitigation of behavioural impacts from a seismic survey and post-event evaluation of sound exposure for individual whales*. *Acoustics 2012 Fremantle: Acoustics, Development and the Environment*, Fremantle, Australia. http://www.acoustics.asn.au/conference_proceedings/AAS2012/papers/p92.pdf.

Warner, G., C. Erbe, and D. Hannay. 2010. Underwater Sound Measurements. (Chapter 3) *In* Reiser, C.M., D.W. Funk, R. Rodrigues, and D. Hannay (eds.). *Marine Mammal Monitoring and Mitigation during Open Water Shallow Hazards and Site Clearance Surveys by Shell Offshore Inc. in the Alaskan Chukchi Sea, July-October 2009: 90-Day Report*. LGL Report P1112-1. Report by LGL Alaska Research Associates Inc. and JASCO Applied Sciences for Shell Offshore Inc., National Marine Fisheries Service (US), and US Fish and Wildlife Service. pp 1-54.

Zhang, Y. and C. Tindle. 1995. Improved equivalent fluid approximations for a low shear speed ocean bottom. *Journal of the Acoustical Society of America* 98(6): 3391-3396. http://scitation.aip.org/content/asa/journal/jasa/98/6/10.1121/1.413789.

Appendix A. Underwater Acoustics Theory and Formulae

A.1. Acoustic Metrics

Underwater sound pressure amplitude is measured in decibels (dB) relative to a fixed reference pressure of p_0 = 1 µPa. Because the perceived loudness of sound, especially impulsive noise such as from seismic airguns, pile driving, and sonar, is not generally proportional to the instantaneous acoustic pressure, several sound level metrics are commonly used to evaluate noise and its effects on marine life. We provide specific definitions of relevant metrics used in the accompanying report. Where possible we follow the ANSI and ISO standard definitions and symbols for sound metrics, but these standards are not always consistent.

The zero-to-peak sound pressure level, or peak sound pressure level (PK; dB re 1 µPa), is the maximum instantaneous sound pressure level in a stated frequency band attained by an acoustic pressure signal, $p(t)$:

$$L_{p,pk} = 20 \log_{10} \left[\frac{\max\left(\left| p(t) \right|\right)}{p_0} \right] \tag{A-1}$$

$L_{p,pk}$ is often included as a criterion for assessing whether a sound is potentially injurious; however, because it does not account for the duration of a noise event, it is generally a poor indicator of perceived loudness.

The sound pressure level (SPL; dB re 1 µPa) is the rms pressure level in a stated frequency band over a specified time window (T, s) containing the acoustic event of interest. It is important to note that SPL always refers to an rms pressure level and therefore not instantaneous pressure:

$$L_p = 10 \log_{10} \left(\frac{1}{T} \int_T p^2(t) dt \Big/ p_0^2 \right) \tag{A-2}$$

The SPL represents a nominal effective continuous sound over the duration of an acoustic event, such as the emission of one acoustic pulse, a marine mammal vocalization, the passage of a vessel, or over a fixed duration. Because the window length, T, is the divisor, events with similar sound exposure level (SEL) but more spread out in time have a lower SPL.

In studies of impulsive noise, the time window T is often defined as the "90% time window" (T_{90}): the period over which cumulative square pressure function passes between 5% and 95% of its full per-pulse value. The SPL computed over this T_{90} interval is commonly called the 90% SPL (SPL(T_{90}); dB re 1 µPa):

$$L_{p90} = 10 \log_{10} \left(\frac{1}{T_{90}} \int_{T_{90}} p^2(t) dt \Big/ p_0^2 \right) \tag{A-3}$$

The sound exposure level (SEL, dB re 1 µPa^2·s) is a measure related to the acoustic energy contained in one or more acoustic events (N). The SEL for a single event is computed from the time-integral of the squared pressure over the full event duration (T):

$$L_E = 10 \log_{10} \left(\int_T p^2(t) dt \Big/ T_0 p_0^2 \right) \tag{A-4}$$

where T_0 is a reference time interval of 1 s. The SEL continues to increase with time when non-zero pressure signals are present. It therefore can be construed as a dose-type measurement, so the

integration time used must be carefully considered in terms of relevance for impact to the exposed recipients.

SEL can be calculated over periods with multiple acoustic events or over a fixed duration. For a fixed duration, the square pressure is integrated over the duration of interest. For multiple events, the SEL can be computed by summing (in linear units) the SEL of the *N* individual events:

$$L_{E,N} = 10\log_{10}\left(\sum_{i=1}^{N} 10^{\frac{L_{E,i}}{10}}\right) \tag{A-5}$$

Because the SPL(T_{90}) and SEL are both computed from the integral of square pressure, these metrics are related by the following expression, which depends only on the duration of the time window *T*:

$$L_p = L_E - 10\log_{10}(T) \tag{A-6}$$

$$L_{p90} = L_E - 10\log_{10}(T_{90}) - 0.458 \tag{A-7}$$

where the 0.458 dB factor accounts for the 10% of SEL missing from the SPL(T_{90}) integration time window.

A.1.1. 1/3-Octave-Band Analysis

The distribution of a sound's power with frequency is described by the sound's spectrum. The sound spectrum can be split into a series of adjacent frequency bands. Splitting a spectrum into 1 Hz wide bands, called passbands, yields the power spectral density of the sound. This splitting of the spectrum into passbands of a constant width of 1 Hz, however, does not represent how animals perceive sound.

Because animals perceive exponential increases in frequency rather than linear increases, analyzing a sound spectrum with passbands that increase exponentially in size better approximates real-world scenarios. In underwater acoustics, a spectrum is commonly split into 1/3-octave-bands, which are one-third of an octave wide; each octave represents a doubling in sound frequency. The center frequency of the *i*th 1/3-octave-band, $f_c(i)$, is defined as:

$$f_c(i) = 10^{i/10}, \tag{A-8}$$

and the low (f_{lo}) and high (f_{hi}) frequency limits of the *i*th 1/3-octave-band are defined as:

$$f_{lo} = 10^{-1/20} f_c(i) \quad \text{and} \quad f_{hi} = 10^{1/20} f_c(i)\ . \tag{A-9}$$

The 1/3-octave-bands become wider with increasing frequency, and on a logarithmic scale the bands appear equally spaced.

The sound pressure level in the *i*th 1/3-octave-band $(L_b^{(i)})$ is computed from the power spectrum $S(f)$ between f_{lo} and f_{hi}:

$$L_b^{(i)} = 10\log_{10}\left(\int_{f_{lo}}^{f_{hi}} S(f)\,df\right) \tag{A-10}$$

Summing the sound pressure level of all the 1/3-octave-bands yields the broadband sound pressure level:

$$\text{Broadband SPL} = 10\log_{10}\sum_{i} 10^{L_b^{(i)}/10} \qquad \text{(A-11)}$$

A.2. Acoustic Models

A.2.1. Pile Driving Source Model

A physical model of pile vibration and near-field sound radiation is used to calculate source levels of piles. The physical model employed in this study computes the underwater vibration and sound radiation of a pile by solving the theoretical equations of motion for axial and radial vibrations of a cylindrical shell. These equations of motion are solved subject to boundary conditions, which describe the forcing function of the hammer at the top of the pile and the soil resistance at the base of the pile (Figure A-1). Damping of the pile vibration due to radiation loading is computed for Mach waves emanating from the pile wall. The equations of motion are discretized using the finite difference (FD) method and are solved on a discrete time and depth mesh.

To model the sound emissions from the piles, the force of the pile driving hammers also had to be modeled. The force at the top of each pile was computed using the GRLWEAP 2010 wave equation model (GRLWEAP, Pile Dynamics 2010), which includes a large database of simulated hammers—both impact and vibratory—based on the manufacturer's specifications. The forcing functions from GRLWEAP were used as inputs to the FD model to compute the resulting pile vibrations.

The sound radiating from the pile itself is simulated using a vertical array of discrete point sources. The point sources are centered on the pile axis. Their amplitudes are derived using an inverse technique, such that their collective particle velocity—calculated using a near-field wave-number integration model—matches the particle velocity in the water at the pile wall. The sound field propagating away from the vertical source array is then calculated using a time-domain acoustic propagation model (Section A.2.3.2). MacGillivray (2014) describes the theory behind the physical model in more detail.

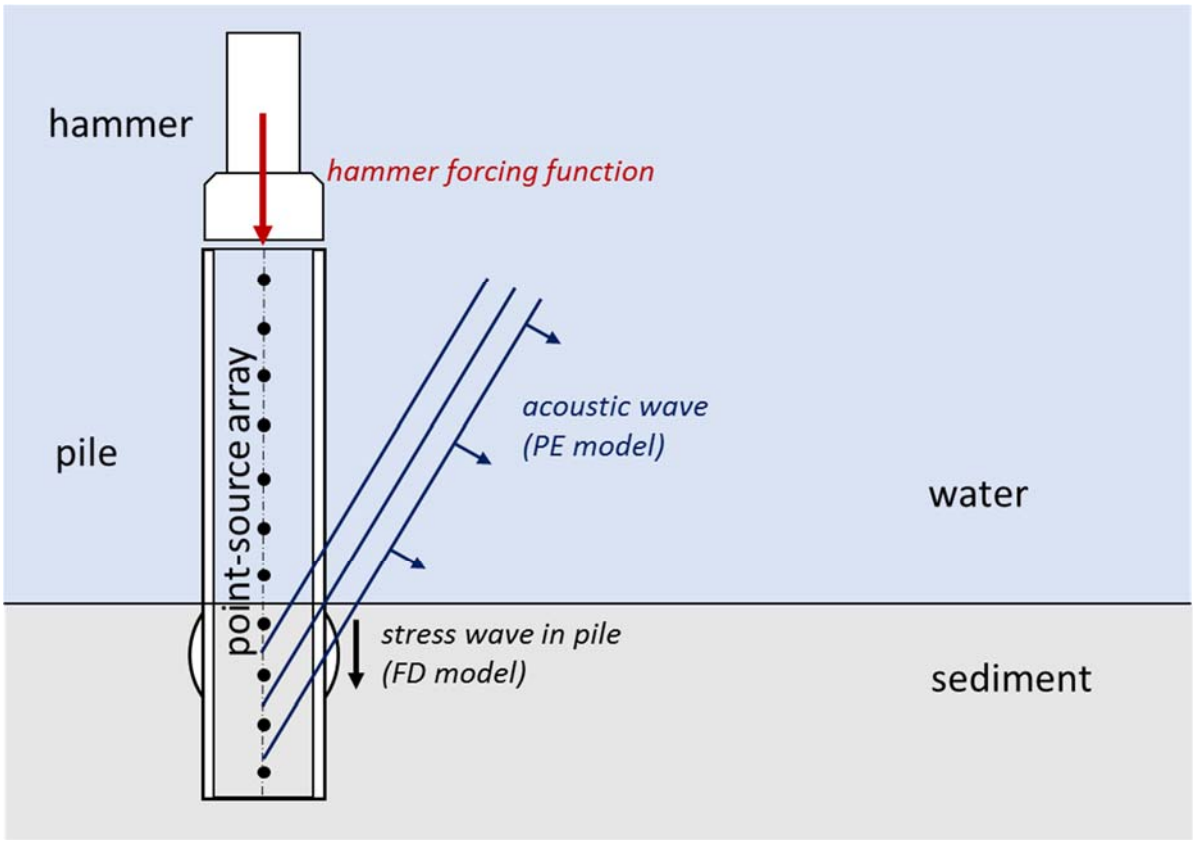

Figure A-1. Physical model geometry for impact driving of a cylindrical pile (vertical cross-section). The hammer forcing function is used with the finite difference (FD) model to compute the stress wave vibration in the pile. A vertical array of point sources is used with the parabolic equation (PE) model to compute the acoustic waves that the pile wall radiates.

A.2.2. Higher-order harmonics in vibratory pile driving

The spectrum of noise measurements corresponding to vibratory pile driving often exhibit significant noise contributions at the fundamental frequency of oscillation of the vibratory hammer, a value typically below 50 Hz. In addition, noise contributions can also be identified at higher frequencies corresponding to multiples of the fundamental frequency. To incorporate this effect into vibratory pile driving using PDSM, the forcing function obtained from GRLWEAP was modified to obtain a distorted forcing function which exhibits higher-frequency content, thereby mimicking the frequency dependence observed in experimental data. The amplitude distortion in this work was implemented in two steps:

- Step 1: the amplitude of the GRLWEAP forcing function was modulated using a non-linear function, causing moderate deformation as shown in the time domain example for the Auke Bay site in Figure A-2. In this example, the chosen non-linear function is the hyperbolic tangent of the amplitude. Note, however, that this specific choice is unimportant for the modelling. The only relevant aspect when selecting the amplitude-distorting function is that the spectrum of the distorted signal exhibits energy at several multiples of the hammer fundamental frequency, as shown in Figure A-2 (top).
- Step 2: Once the non-linear distortion was applied, the spectrum of the resulting forcing function was detrended by subtracting the local mean, and then multiplied by the function H(f) shown in Figure A-2 (top), which leaves the spectrum unaltered below 55 Hz, and enforces a decay trend of 55 dB/decade at frequencies higher than 55 Hz. The shape and trend of H(f) was selected by

trial and error, running the vibratory model at Auke Bay, Kake, and Ketchikan until the modeled band levels where within reasonable agreement to those measured at the closest range.

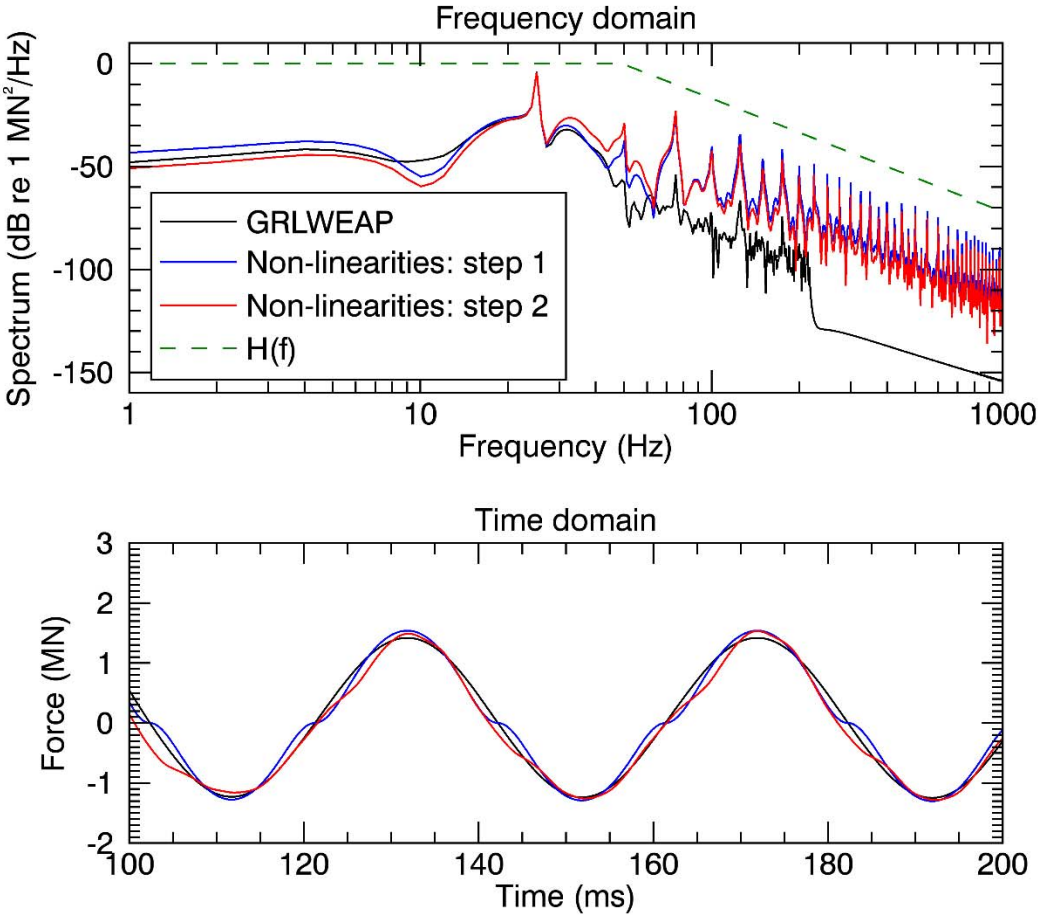

Figure A-2. Effects of introducing non-linearities to the forcing function for vibratory pile driving at Auke Bay, shown in the frequency (top) and time (bottom) domains. The procedure was applied to all vibratory pile driving modelling in this report.

A.2.3. Sound Propagation Models

A.2.3.1. Sound Propagation with MONM

Underwater sound propagation (i.e., transmission loss) at frequencies of 10 Hz to 5 kHz was predicted with JASCO's Marine Operations Noise Model (MONM). MONM computes received per-pulse SEL for directional impulsive sources, and SEL over 1 s for non-impulsive sources, at a specified source depth.

MONM computes acoustic propagation via a wide-angle parabolic equation solution to the acoustic wave equation (Collins 1993) based on a version of the U.S. Naval Research Laboratory's Range-dependent Acoustic Model (RAM), which has been modified to account for a solid seabed (Zhang and Tindle 1995). The parabolic equation method has been extensively benchmarked and is widely employed in the underwater acoustics community (Collins et al. 1996). MONM accounts for the additional reflection loss at the seabed, which results from partial conversion of incident compressional waves to shear waves at the seabed and sub-bottom interfaces, and it includes wave attenuations in all layers. MONM incorporates

the following site-specific environmental properties: a bathymetric grid of the modeled area, underwater sound speed as a function of depth, and a geoacoustic profile based on the overall stratified composition of the seafloor.

MONM computes acoustic fields in three dimensions by modeling transmission loss within two-dimensional (2-D) vertical planes aligned along radials covering a 360° swath from the source, an approach commonly referred to as N×2-D. These vertical radial planes are separated by an angular step size of $\Delta\theta$, yielding N = 360°/$\Delta\theta$ number of planes (Figure A-3).

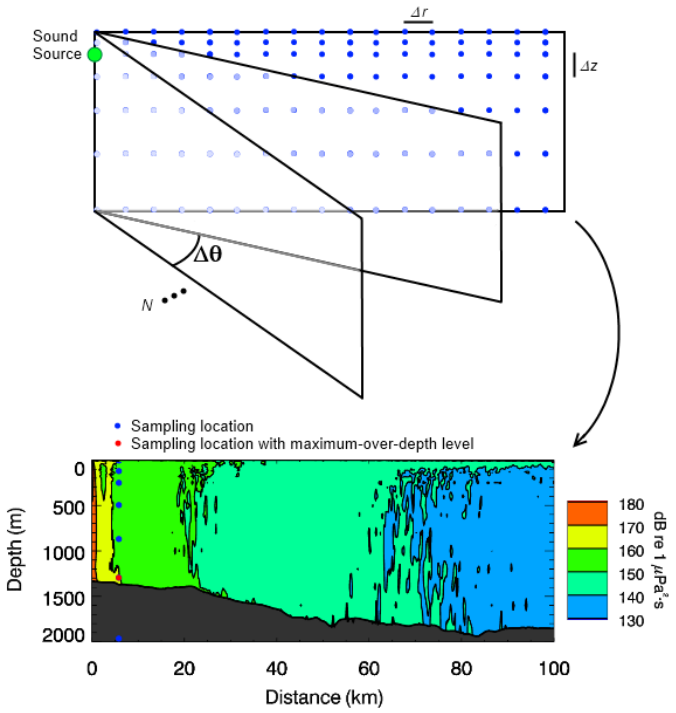

Figure A-3. The N×2-D and maximum-over-depth modeling approach used by MONM.

MONM treats frequency dependence by computing acoustic transmission loss at the center frequencies of 1/3-octave-bands. Sufficiently many 1/3-octave-bands, starting at 10 Hz, are modeled to include the majority of acoustic energy emitted by the source. At each center frequency, the transmission loss is modeled within each of the N vertical planes as a function of depth and range from the source. The 1/3-octave-band received per-pulse SELs are computed by subtracting the band transmission loss values from the directional source level in that frequency band. Composite broadband received SELs are then computed by summing the received 1/3-octave-band levels.

The received per-pulse SEL sound field within each vertical radial plane is sampled at various ranges from the source, generally with a fixed radial step size. At each sampling range along the surface, the sound field is sampled at various depths, with the step size between samples increasing with depth below the surface. The step sizes are chosen to provide increased coverage near the depth of the source and at depths of interest in terms of the sound speed profile. The received per-pulse SEL at a surface sampling location is taken as the maximum value that occurs over all samples within the water column, i.e., the maximum-over-depth received per-pulse SEL. These maximum-over-depth per-pulse SELs are presented as color contours around the source.

MONM's predictions have been validated against experimental data from several underwater acoustic measurement programs conducted by JASCO (Hannay and Racca 2005, Aerts et al. 2008, Funk et al. 2008, Ireland et al. 2009, O'Neill et al. 2010, Warner et al. 2010, Racca et al. 2012a, Racca et al. 2012b, Martin et al. 2015).

A.2.3.2. Sound Propagation with FWRAM

For impulsive sounds from impact pile driving, time-domain representations of the pressure waves generated in the water are required to calculate SPL and peak pressure level. Furthermore, the pile must be represented as a distributed source to accurately characterize vertical directivity effects in the near-field zone. For this study, synthetic pressure waveforms were computed using FWRAM, which is a time-domain acoustic model based on the same wide-angle parabolic equation (PE) algorithm as MONM. FWRAM computes synthetic pressure waveforms versus range and depth for range-varying marine acoustic environments, and it takes the same environmental inputs as MONM (bathymetry, water sound speed profile, and seabed geoacoustic profile). Unlike MONM, FWRAM computes pressure waveforms via Fourier synthesis of the modeled acoustic transfer function in closely spaced frequency bands. FWRAM employs the array starter method to accurately model sound propagation from a spatially distributed source (MacGillivray and Chapman 2012). Besides providing direct calculations of the peak pressure level and SPL, the synthetic waveforms from FWRAM can also be used to convert the SEL values from MONM to SPL

Appendix B. Threshold Criteria for Marine Mammal Injury (Level A) and Behavioral Disturbance (Level B)

Determining standards to quantify the way in which underwater noise can affect marine fauna is an active research topic. There are different views among bioacousticians about the best method to estimate injury and disturbance effects on animals, and because evaluating chronic effects is even more complex and harder to quantify, there is little consensus at the moment on how to perform those assessments. The criteria applied in this study are based on references that represent the current best available science, and require computing peak pressure level (PK), sound pressure level (SPL), and sound exposure level (SEL). Appendix A.1 describes these metrics and provides formulae. Since 2007, several expert groups have investigated an SEL-based assessment approach for injury, publishing some key papers on the topic; the number of studies investigating the level of disturbance to marine animals by underwater noise has also increased substantially.

Results of this modeling study are presented in terms of the following noise criteria:

- Dual criteria (Auditory-weighted SEL and PK) Level A thresholds for marine mammals, based on NMFS (2016) for all sound sources.
- Level B thresholds for marine mammals, based on the interim NMFS criteria (NMFS 2013) of 120dB re 1 µPa SPL for non-impulsive and 160 dB re 1 µPa SPL for impulsive sound sources.

B.1. Auditory Weighting Functions for Marine Mammals

The potential for noise to affect animals depends on how well the animals can hear it. Noises are less likely to disturb or injure an animal if they are at frequencies that the animal cannot hear well. An exception occurs when the sound pressure is so high that it can physically injure an animal by non-auditory means (i.e., barotrauma). For sound levels below such extremes, the importance of sound components at particular frequencies can be scaled by frequency weighting relevant to an animal's sensitivity to those frequencies (Nedwell and Turnpenny 1998, Nedwell et al. 2007).

In 2015, a U.S. Navy technical report by Finneran (2015) recommended new auditory weighting functions. The overall shape of the auditory weighting functions is similar to human A-weighting functions, which follows the sensitivity of the human ear at low sound levels. The new frequency-weighting function is expressed as:

$$G(f) = K + 10\log_{10}\left[\left(\frac{(f/f_{lo})^{2a}}{\left[1+(f/f_{lo})^{2}\right]^{a}\left[1+(f/f_{hi})^{2}\right]^{b}}\right)\right] \quad \text{(B-1)}$$

Finneran (2015) proposed five functional hearing groups for marine mammals in water: low-, mid-, and high-frequency cetaceans, phocid pinnipeds, and otariid pinnipeds. The parameters for these frequency-weighting functions were further modified the following year (Finneran 2016) and were adopted in NOAA's technical guidance that assesses noise impacts on marine mammals (NMFS 2016). Table B-1 lists the frequency-weighting parameters for each hearing group; Figure B-1. shows the resulting frequency-weighting curves.

Table B-1. Parameters for the auditory weighting functions recommended by NMFS (2016).

Hearing group	*a*	*b*	f_{lo} (Hz)	f_{hi} (kHz)	*K* (dB)
Low-frequency cetaceans	1.0	2	200	19,000	0.13
Mid-frequency cetaceans	1.6	2	8,800	110,000	1.20

Hearing group	*a*	*b*	f_{lo} (Hz)	f_{hi} (kHz)	*K* (dB)
High-frequency cetaceans	1.8	2	12,000	140,000	1.36
Phocid pinnipeds in water	1.0	2	1,900	30,000	0.75
Otariid pinnipeds in water	2.0	2	940	25,000	0.64

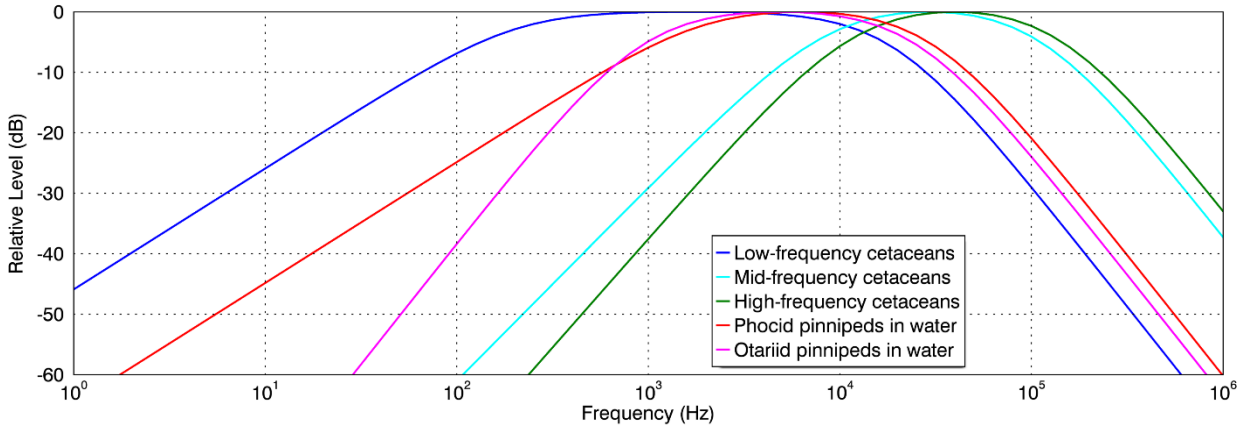

Figure B-1. Auditory weighting functions for functional marine mammal hearing groups as recommended by NMFS (2016).

B.2. Auditory injury (Level A) Threshold Criteria for Marine Mammals

The latest National Oceanic and Atmospheric Administration (NOAA) criteria for injury (NMFS 2016) and its earlier iterations (NOAA 2013, 2015) have been scrutinized by the public, industrial proponents, and academics. This study applied the specific methods and Level A thresholds summarized by NMFS (2016, Table B-2). The Level A criteria provide cautionary estimates of levels above which acoustic exposure could lead to hearing loss, a process known as permanent hearing threshold shift (PTS).

Table B-2. Marine mammal Level A thresholds based on NMFS (2016) peak pressure level in dB re 1 µPa, and auditory-weighted SEL (24 h) in dB re 1 µPa²·s.

Hearing group	Impulsive source		Non-impulsive source
	Peak pressure level (dB re 1 µPa)	Auditory-weighted SEL_{24h} (dB re 1 µPa²·s)	Auditory-weighted SEL_{24h} (dB re 1 µPa²·s)
Low-frequency cetaceans	219	183	199
Mid-frequency cetaceans	230	185	198
High-frequency cetaceans	202	155	173
Phocid pinnipeds in water	218	185	201
Otariid pinnipeds in water	232	203	219

B.3. Disturbance (Level B) Threshold Criteria for Marine Mammals

In this assessment we applied the interim NMFS criteria (NMFS 2013) because these are the most recently published disturbance criteria for marine mammals (Table B-3).

Table B-3. Marine mammal Level B thresholds (SPL, dB re 1 µPa).

Impulsive source	Non-impulsive source
160	120

Appendix C. **Modeling Considering High Shear Velocity in Bedrock Substrate**

The data collected at Kodiak during impact and vibratory pile driving exhibit a pronounced spectral-notch at frequencies between 90 Hz and 200 Hz (Denes et al. 2016). In modeled band levels (Figure 12), a notch for impact pile driving is also visible, although it is much less pronounced compared to the notches in the measurements. This discrepancy between the model and the data, combined with evident notches in both vibratory and impact pile driving, suggest that the interaction between the pile-generated noise and the seabed as the cause.

This section explains the spectral notch observed at Kodiak, based on three observations:

- The bedrock at Kodiak was relatively shallow compared to other sites, and the overburden sediments at the site were 15 to 20 feet thick.
- Unlike other cases in the literature, where piles are forced into fractured bedrock by impact driving, piles at Kodiak had to be drilled in, which suggests consolidated as opposed to fractured bedrock.
- Noise due to impact or vibratory pile driving propagates into the water as a Mach cone, and impinges the seabed with a grazing angle of around 17°, as determined by the speed of sound in steel (the pile material) and water.

Sound that propagates in environments where the seafloor consists of consolidated bedrock can exhibit similar notches at selective frequencies (Duncan et al. 2009) because the compressional waves that propagate through the water transform into shear waves that propagate through the bedrock. To investigate the hypothesis that the notches in the frequency spectrum from the data at Kodiak are a result of such shear wave transformations, we examined the plane-wave, seabed reflection coefficient (Figure C-1) corresponding to the geoacoustic parameters from Kodiak, but we adjusted the shear speed to 1300 m/s for the bedrock layer. By considering shear propagation, the reflection coefficient for a grazing angle of 17° has a magnitude between 0.1 and 0.4 at frequencies below 200 Hz. This means that sounds at these frequencies would be attenuated and this might explain the reduction in pile driving noise levels at that frequency range.

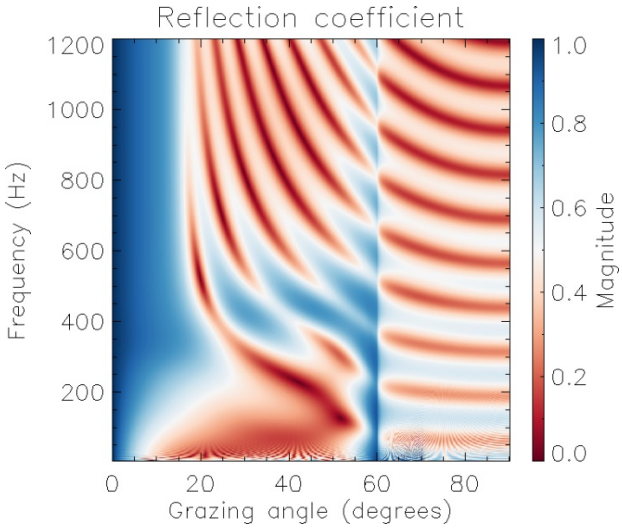

Figure C-1 Kodiak: Plane-wave seabed reflection coefficient, considering shear sound speed of 1300 m/s for the bedrock layer.

At the time of this work, acoustic propagation models that can handle high shear speed velocities, and can compute sound levels over a few kilometers at a reasonable computational speed, were not

available. So we investigated the impact of shear speed on received levels by adjusting the equivalent pile-driving monopoles for impact and vibratory pile driving. This adjustment consisted of reducing the amplitude in the water and sediment borne monopoles using the frequency-dependent amplitude of the seabed reflection coefficient at a grazing angle of 17°, since most of the pile driving noise impinges the seabed at this angle. When using the adjusted pile driving signatures in FWRAM, the notch in the frequency spectrum better matches the observed data (Figure C-2). The sound generated by the pile is reduced in this case, meaning that the sound levels at a given range are lower than those computed using the unadjusted source monopoles (Figure C-3 and Figure C-4).

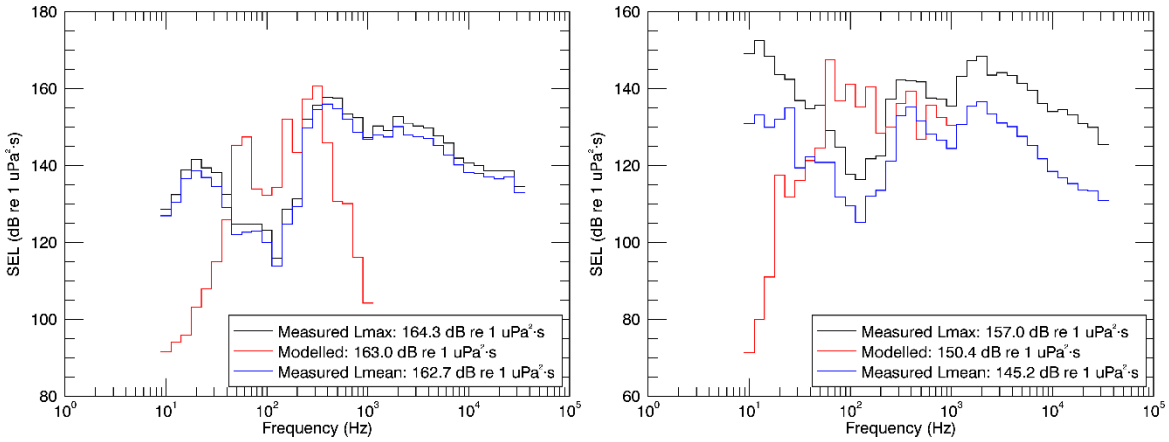

Figure C-2 Kodiak: Modeled band labels for (left) impact and (right) vibratory pile driving at the closest measurement range, compared to measured band levels (maximum and mean). Modeled levels were obtained by considering high shear sound speed in the seabed.

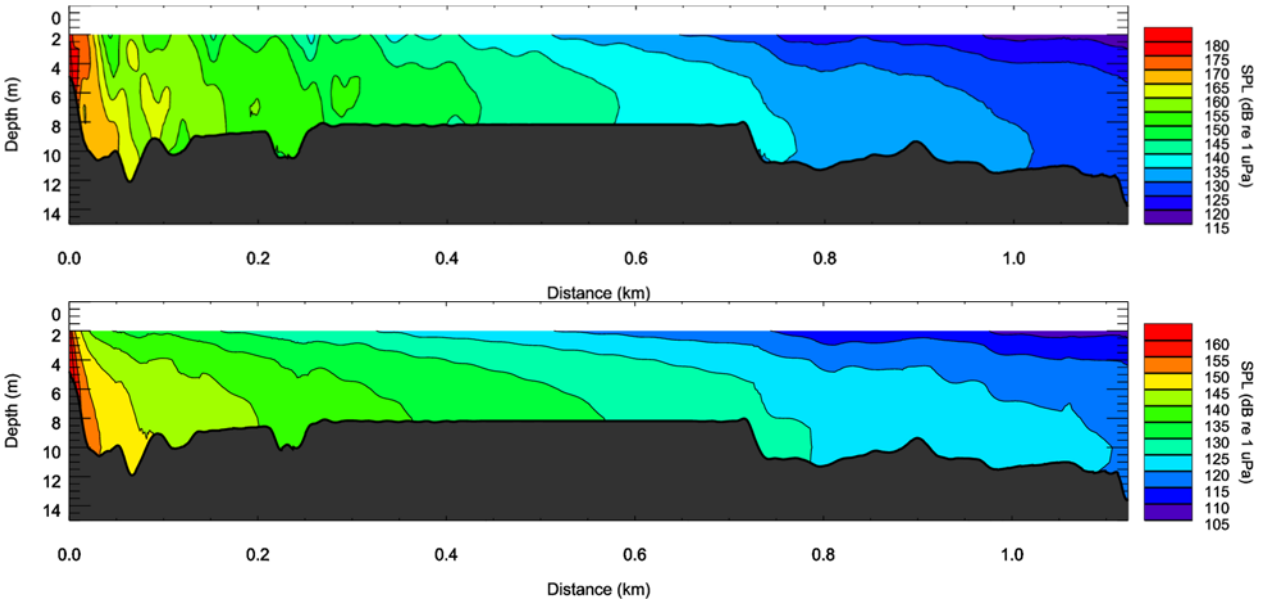

Figure C-3 Kodiak: Spatial dependency of the modeled SPL for (top) impact and (bottom) vibratory pile driving considering high shear sound speed, along a transect from the pile in the direction of the furthest measurement point. The bathymetry along the selected transect is shown using black shading.

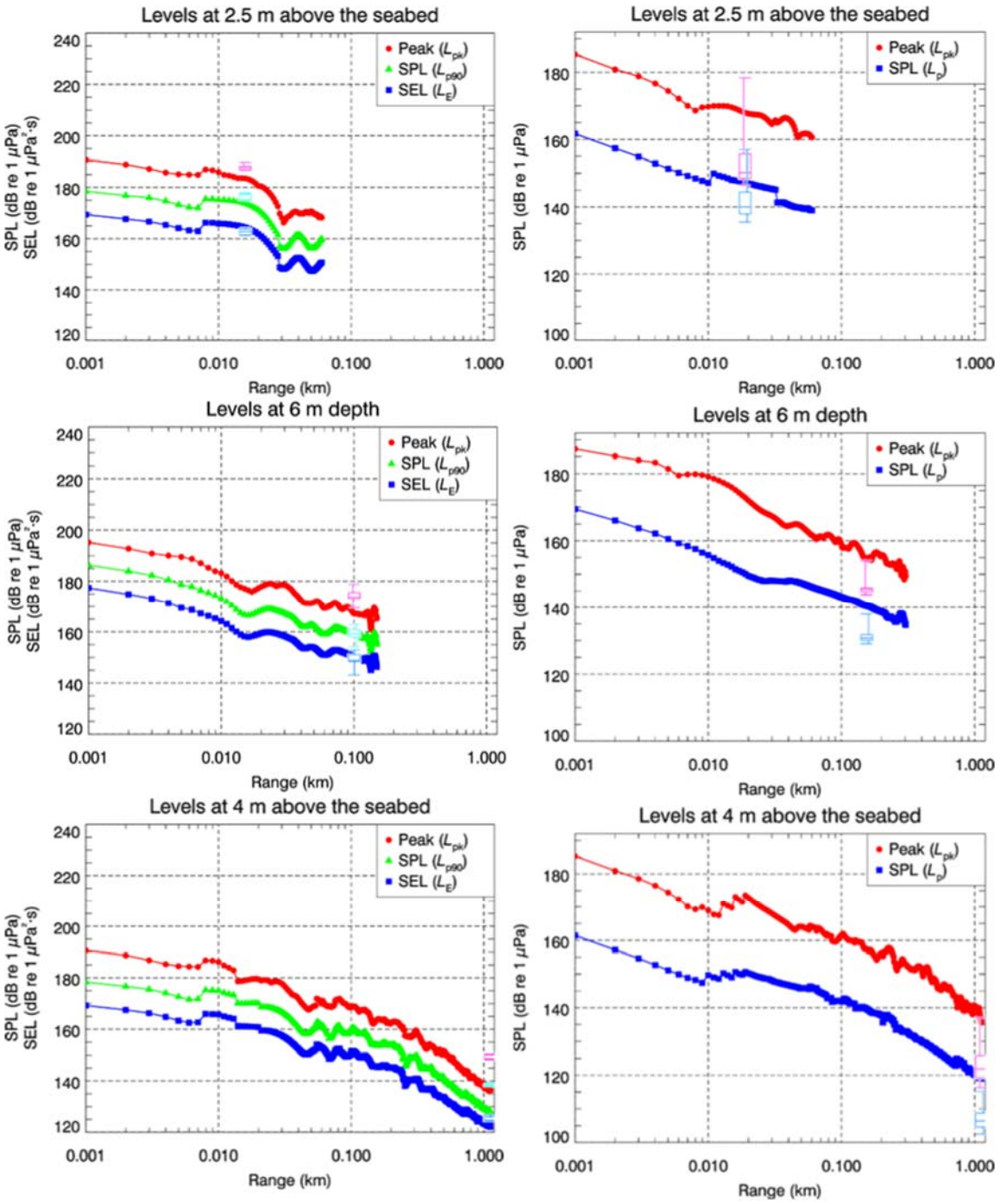

Figure C-4 Kodiak: Comparison of modeled and measured SEL, SPL, and PK levels (left column) impact and (right column) vibratory pile driving, considering high shear sound speed. The ranges for the measurements are about 7 m (top row), 300 m (middle row), and 1200 m (bottom row). The measured data is presented as in the box-and-whisker format in light blue, indigo, and magenta for SEL, SPL, and PK levels, respectively.